HHS Public Access

Author manuscript

J Geophys Res Atmos. Author manuscript; available in PMC 2020 February 05.

Published in final edited form as:

J Geophys Res Atmos. 2018 April 16; 123(7): 3704–3723. doi:10.1002/2017JD027900.

Characteristic Vertical Profiles of Cloud Water Composition in Marine Stratocumulus Clouds and Relationships With Precipitation

Alexander B. MacDonald[1], **Hossein Dadashazar**[1], **Patrick Y. Chuang**[2], **Ewan Crosbie**[3,4], **Hailong Wang**[5], **Zhen Wang**[1], **Haflidi H. Jonsson**[6], **Richard C. Flagan**[7], **John H. Seinfeld**[7], **Armin Sorooshian**[1,8]

[1]Department of Chemical and Environmental Engineering, University of Arizona, Tucson, AZ, USA

[2]Earth and Planetary Sciences, University of California, Santa Cruz, CA, USA

[3]Science Systems and Applications, Inc., Hampton, VA, USA

[4]NASA Langley Research Center, Hampton, VA, USA

[5]Atmospheric Sciences and Global Change Division, Pacific Northwest National Laboratory, Richland, WA, USA

[6]Department of Meteorology, Naval Postgraduate School, Monterey, CA, USA

[7]Department of Chemical Engineering, California Institute of Technology, Pasadena, CA, USA

[8]Department of Hydrology and Atmospheric Sciences, University of Arizona, Tucson, AZ, USA

Abstract

This study uses airborne cloud water composition measurements to characterize the vertical structure of air-equivalent mass concentrations of water-soluble species in marine stratocumulus clouds off the California coast. A total of 385 cloud water samples were collected in the months of July and August between 2011 and 2016 and analyzed for water-soluble ionic and elemental composition. Three characteristic profiles emerge: (i) a reduction of concentration with in-cloud altitude for particulate species directly emitted from sources below cloud without in-cloud sources (e.g., Cl^- and Na^+), (ii) an increase of concentration with in-cloud altitude (e.g., NO_2^- and formate), and (iii) species exhibiting a peak in concentration in the middle of cloud (e.g., non-sea-salt SO_4^{2-}, NO_3^-, and organic acids). Vertical profiles of rainout parameters such as loss frequency, lifetime, and change in concentration with respect to time show that the scavenging efficiency throughout the cloud depth depends strongly on the thickness of the cloud. Thin clouds exhibit a greater scavenging loss frequency at cloud top, while thick clouds have a greater scavenging loss frequency at cloud base. The implications of these results for treatment of wet scavenging in models are discussed.

Correspondence to: A. Sorooshian,armin@email.arizona.edu

1. Introduction

Clouds are a key agent in the planet's energy budget, the hydrological cycle, transferring nutrients, and contaminants from one area to another via nucleation scavenging and eventual rainout, chemical transformations of gases and particles, and vertical redistribution of airborne material. Quantifying the nature and magnitude of these cloud processes is challenging owing to measurement limitations. Application of chemical tracers presents a potentially effective means to understand cloud processes such as wet scavenging, the removal of gases, and particles from the atmosphere by cloud droplets and rain drops (Lamb & Verlinde, 2011).

The majority of cloud water field studies have focused on composition and sources of gaseous and particulate material affecting clouds in regions such as Asia (Desyateriket al., 2013; Ghauri et al., 2001; Li et al., 2017; X. H. Liu et al., 2012; Sun et al., 2010,2015; Watanabe et al., 2001), North America (Bator & Collett, 1997; Boone et al., 2015; Collett et al., 1994; Deininger & Saxena, 1997; Hayden et al., 2008; Hutchings et al., 2008; Leaitch et al., 1992; Malcolm et al., 2003; Munger et al., 1989a; Pratt et al., 2013; Rao & Collett, 1998; Weathers et al., 1988), Europe (Cini et al., 2002; Fomba et al., 2015; Lammel, 1995; Marinoni et al., 2004; Plessow et al., 2001; Polkowska et al., 2014; Sedlak et al., 1997; van Pinxteren et al., 2016; Wieprecht et al., 2005; Wilkinson et al., 1997), the Caribbean Islands (Gioda et al., 2008, 2009, 2013), and over marine areas (Benedict et al., 2012; Crahan et al., 2004; Hegg et al., 2002; Prabhakar et al., 2014; Sorooshian, Wang, Coggon, et al., 2013; Sorooshian et al., 2015; Straub et al., 2007; Wang et al., 2014; Youn et al., 2015). Vertically resolved cloud water data are scarce and have focused on continental orographic clouds (Fowler et al., 1988; Kins et al., 1988) and cumulus clouds (Leaitch et al., 1983). To our knowledge, the variation of cloud water concentration of dissolved species in marine stratocumulus clouds has not been studied. Such information could be useful for understanding wet scavenging processes in clouds in the marine boundary layer.

Wet scavenging comprises two microphysical processes: (i) the activation of particles to form cloud droplets (termed nucleation scavenging) and (ii) the incorporation of particles and gases into existing droplets (particles enter droplets by impaction and diffusion, whereas gases are partitioned into droplets by diffusion). It is also convenient to classify wet scavenging on the macrophysical scale according to whether it occurs in or below clouds. In-cloud scavenging (also called rainout) is the removal of chemical species from a cloud volume via precipitating rain drops exiting the cloud at cloud base; these species could have entered the rain drops by either (i) seeding cloud droplets via nucleation scavenging, which then undergo collision-coalescence to form rain drops, or (ii) entering cloud droplets or rain drops via impaction and diffusion processes. Below-cloud scavenging (also called washout) is the removal of chemical species from an air volume located below cloud base by precipitating rain drops (Garrett et al., 2006; Neu & Prather, 2012; Seinfeld & Pandis, 2016; Wang et al., 2013). The relative importance of in-cloud and below-cloud scavenging in removing a chemical species from the atmosphere depends on the meteorological conditions and the properties of the species; for example, rainout is the main sink for cloud condensation nuclei (CCN) and particles in the accumulation mode (Barth et al., 2000; Ervens, 2015; Wood, 2006), the rate of rainout of nitric acid (HNO_3) is an order of

magnitude greater than that of washout (Garrett et al., 2006), and washout is greater for soluble gases than for aerosols because there is a greater concentration of the former below the cloud (Gong et al., 2011). The microphysical scavenging processes of nucleation, impaction, and diffusion transfer species from the interstitial air phase into the aqueous phase, whereas (in the absence of evaporation of precipitating rain drops) the macrophysical processes of rainout and washout transfer species from the atmosphere onto the Earth's surface. This study will focus on the removal of species from a cloud due to the loss of dissolved species contained in precipitating rain drops exiting the cloud (i.e., rainout).

The aim of this work is to use vertically resolved stratocumulus cloud water composition data collected off the California coast to address the following questions: (i) what are characteristic in-cloud vertical concentration profiles for a group of constituent species? and (ii) how are in-cloud vertical concentration profiles related to profiles of precipitation? The results of this work have important implications not only for characterizing cloud water composition but also for understanding the governing factors removing gases and particles from the marine boundary layer.

2. Experimental Methods

2.1 Field Campaigns

This study analyzes a comprehensive set of cloud water samples obtained in the stratocumulus cloud deck off the California coast during the months of July and August between 2011 and 2016. The Center for Interdisciplinary Remotely-Piloted Aircraft Studies Twin Otter conducted flights in the following four campaigns from which data are analyzed: the Eastern Pacific Emitted Aerosol Cloud Experiment (E-PEACE) (Russell et al., 2013; Wonaschütz et al., 2013), the Nucleation in California Experiment (NiCE) (Crosbie et al., 2016; Maudlin et al., 2015), the Biological and Oceanic Atmospheric Study (BOAS) (Wang et al., 2016), and the Fog and Stratocumulus Evolution (FASE) Experiment (Dadashazar et al., 2017; Schlosser et al., 2017). Table 1 summarizes the dates and flights for these field experiments, while Figure 1 shows the spatial area of the flight tracks during each experiment. Based out of Marina, California, flights lasted ~4–4.5 hr with maneuvers usually including vertical soundings and level legs at the following altitudes relative to the cloud deck: near surface (>50 m above sea level), immediately below cloud base, above cloud base, midcloud, below cloud top, immediately above cloud top, and >100 m above cloud top in the free troposphere. Vertical profiles of cloud properties were collected in relatively small horizontal distances, typically being between 10 and 30 km. The payload was similar in each of these campaigns with instruments relevant to this study summarized below.

2.2. Cloud Water Data

Cloud water was collected using a modified Mohnen slotted-rod collector (Hegg & Hobbs, 1986), which was manually deployed out the top of the Twin Otter when in cloud. The collector was cleaned at the beginning of each research flight (RF) by rinsing it with copious amounts of Milli-Q water. After cleaning, blank samples of Milli-Q water were collected. During flight, cloud water is collected preferentially over rain water, the result of droplets

colliding and coalescing into larger drops (radii ≳ 25 μm) (Sorooshian, Wang, Feingold, et al., 2013; Wang & Feingold, 2009), due to large rain drops shattering upon impact with the collector. Furthermore, it is worth cautioning that the Mohnen slotted-rod collector does not collect all cloud droplet sizes equally (Hegg & Hobbs, 1986); since the cloud droplet composition varies across droplet size (Bator & Collett, 1997), the cloud water composition will be biased. Samples were collected in high-density polyethylene bottles over a typical duration of ~5–30 min and immediately stored in a cooler at a nominal 5 °C (to slow chemical and biological activity) until laboratory analysis. Each liquid sample was then split into numerous fractions for the following types of analyses: (i) pH (Thermo Scientific Orion 9110DJWP Combination Semi-Micro pH Electrode (E-PEACE, NiCE, BOAS) and Thermo Scientific Orion 8103BNUWP Ross Ultra Semi-Micro pH probe (FASE), both calibrated with 4.01 and 7.00 pH buffer solutions); (ii) water-soluble ionic composition (ion chromatography, IC; Thermo Scientific Dionex ICS-2100 system); and (iii) water-soluble elemental composition (inductively coupled plasma mass spectrometry (ICP-MS; Agilent 7700 Series) for E-PEACE, NiCE, and BOAS; triple quadrupole inductively coupled plasma mass spectrometry (ICP-QQQ; Agilent 8800 Series) for FASE). The dual IC system includes AS11-HC (2 × 250 mm) and CS12A (2 × 250 mm) columns for anion and cation analysis, respectively. Anion IC analysis was conducted with a multistep gradient using potassium hydroxide eluent. Cation IC analysis was conducted with an isocratic method using methanesulfonic acid eluent. Almost all the cloud water samples were free from visible solids; the few samples that had solids were decanted when they were poured into the vial being fed to the ICP-MS, thus permitting the analysis of the water soluble fraction of elements. Table S1 lists the 29 ions and 46 elements measured, in addition to the limit of detection of the relevant species for this study.

To account for the dilution of a soluble species due to droplet size, aqueous concentrations are converted to air-equivalent concentrations using the sample-averaged liquid water content (LWC; $\text{mass}_{\text{water}}\ \text{volume}_{\text{air}}^{-1}$), as measured by a PVM-100A probe (Gerber et al., 1994). In accordance with previous cloud-focused studies in the region, a threshold LWC value of 0.02 g m^{-3} was used to distinguish between cloudy and cloud-free air (Prabhakar et al., 2014; Wang et al., 2014). Non–sea-salt sulfate (NSS SO_4^{2-}) concentration was calculated using the relative abundance of SO_4^{2-} to sodium (Na^+) in natural sea salt (Seinfeld & Pandis, 2016), with the assumption that Na^+ derives entirely from sea salt in the study region. Sodium data are used from ICP-MS analysis as compared to IC due to having more data points (some ions, including Na^+, could not be measured with IC for E-PEACE).

2.3. Supplementary Airborne Measurements and Calculations

To assist in the interpretation of the cloud water data, numerous other Twin Otter instrument data are used. All cloud and meteorological data (e.g., temperature, humidity, and winds) are synchronized at 1 Hz time resolution. The LWC data set is used to define cloud base and top altitudes using the aforementioned 0.02 g m^{-3} threshold. Rain rate (R, length time^{-1}, mm day^{-1}) is calculated based on documented methods (e.g., Chen et al., 2012; Dadashazar et al., 2018; Feingold et al., 2013) as follows:

$$R = \int \frac{4}{3} \pi r^3 v(r) n \, dr \quad (1)$$

where r is the radius of the drop (length), $v(r)$ is the drop fall velocity (length time^{-1}) for a given drop size, n is the drop number distribution (length^{-1} volume^{-1}), and $n\,dr$ is the drop count (volume^{-1}) in the bin of width dr (length). The vertically resolved drop number distribution is obtained using a Cloud Imaging Probe (D_p ~ 25−1,550 μm). The value of $v(r)$ is approximated by fitting the drop fall velocities reported by Gunn and Kinzer (1949) to the equations provided in Feingold et al. (2013). The limits of integration include drizzle drop radii ($20 < r < 400$ μm) (Wood, 2012) all the way to the upper limit of Cloud Imaging Probe (1,550 μm). The rain rates analyzed in this study (in section 4.2) are not negligible ($R > 0.1$ mm day^{-1}) (Stephens & Haynes, 2007) and correspond to light and moderate drizzle (where light: $R < 0.5$ mm day^{-1}; moderate: $0.5 < R < 2$ mm day^{-1}; heavy: $R > 2$ mm day^{-1}; Wood, 2012). Consequently, nondrizzling clouds are omitted in this study.

It is important to distinguish clouds that are decoupled versus coupled from the surface layer, as the chemical composition of their droplets will reflect this difference (Wang et al., 2016). We follow the methods employed in Wang et al. (2016) to distinguish between the two types of clouds based on discontinuities in thermodynamic variables obtained from vertical sounding data. The majority of cloud water samples (96%) were obtained from clouds coupled to the surface layer, which is the focus of this work (i.e., decoupled clouds were omitted from this study). The range of cloud conditions associated with the collected samples from coupled clouds is as follows: $R = 0.03$−3.69 mm day^{-1}, cloud depth = 38–728 m, and cloud base height = 69–900 m.

2.4. Constructing Vertical Profiles

Two approaches are used to create vertical profiles of cloud water composition. The first approach, termed the “case study approach,” uses cloud water samples collected in a sequential pattern of level legs above each other in thin altitude bins (example in Figure S1). Owing to challenges with collecting samples using this approach, only 45 of the 385 total samples, representing 11 profiles, were obtained. An example of a challenge included the high time demand level legs required at multiple levels in cloud while needing to meet other scientific objectives requiring other patterns in flight. The second approach, termed the “cumulative approach,” uses vertically binned concentration averages of all samples collected throughout the four missions based on mean altitude of each sample over the duration of its collection, even if the aircraft flew across the entire depth of a cloud during the collection of one sample. Fora given species, the case study approach produces 11 individual vertical profiles, whereas the cumulative approach produces a single vertical profile.

In both approaches, the mean altitude during sample collection is calculated for periods when LWC ≥ 0.02 g m^{-3}. This mean altitude is then converted to normalized cloud height with knowledge of cloud base and top height (i.e., base = 0, top = 1). Vertical concentration profiles of eight chemical species are analyzed: sodium (Na^+), chloride (Cl^-), nitrate (NO_3^-), NSS SO_4^{2-}, methanesulfonate (MSA), oxalate, nitrite (NO_2^-), and formate. These

species are either directly emitted or secondarily produced and are influenced by varying degrees from different emission sources. For both approaches, it is cautioned that the number of cloud water samples collected in each vertical bin varied due to the uneven amount of sampling time spent in each vertical bin, which is a result of the difficulty of accumulating sufficient sample volume in the vertical bins with the lowest LWC values (i.e., typically at cloud base). The statistical consequences of uneven vertical sampling are discussed in section 4.1.2.

3. Wet Scavenging

Wet scavenging is the main atmospheric removal process for submicrometer particles and many soluble gases (Ervens, 2015), thus being crucial in calculations of (i) the vertical profile of gases and particles in the atmosphere, (ii) the atmospheric residence time of species and therefore the distance they can travel from sources (Wang et al., 2013), and (iii) air quality. Wet scavenging is, however, challenging to describe quantitatively (Seinfeld & Pandis, 2016), thus creating a major source of uncertainty in climate models (Neu & Prather, 2012; Wang et al., 2013).

A number of climate models, such as the Community Atmospheric Model version 5 (CAM5), simulate both the rainout and washout components of wet scavenging in stratiform and convective clouds (X. Liu et al., 2012; Neale et al., 2012). Given that it is neither feasible nor practical to explicitly represent processes of very different spatial and temporal scale in a single climate model, many relevant chemical, microphysical, and dynamical processes are highly parameterized (Ervens, 2015). The complexity of wet scavenging has led to the development of various parameters that relate species concentrations and meteorological conditions. One such parameter is the mass scavenging efficiency of a species S, α (dimensionless). For an unreactive species S, α is defined as the fraction of total (dissolved plus interstitial) species S that is dissolved in droplets (Daum et al., 1984):

$$\alpha = \frac{[S]_{\mathrm{dis,air}}}{[S]_{\mathrm{tot,air}}} = \frac{[S]_{\mathrm{dis,air}}}{[S]_{\mathrm{dis,air}} + [S]_{\mathrm{int,air}}} \tag{2}$$

The subscripts dis, int, and tot stand for dissolved, interstitial, and total, respectively. The subscript air stands for air-equivalent concentration ($\mathrm{mass_{solute}\ volume_{air}^{-1}}$) and is related to the cloud droplet concentration ($\mathrm{mass_{Solute}\ volume_{droplet}^{-1}}$) as follows:

$$[S]_{\mathrm{dis,cloud}} = \frac{\rho_w}{LWC}[S]_{\mathrm{disair}} \tag{3}$$

Where ρ_w is the density of liquid water ($\mathrm{mass_{water}\ volume_{water}^{-1}}$). For reactive species that are formed within cloud droplets, $[S]_{\mathrm{int,\ air}}$ in equation (2) must account for both the interstitial species S and the interstitial gaseous precursors of species S. Many climate models calculate α for stratiform clouds by explicitly predicting the fraction of particles that activate into droplets (e.g., Barth et al., 2000; Easter et al., 2004; X. Liu et al., 2012). The activated fraction depends on maximum in-cloud supersaturation and particle properties

such as size and hygroscopicity. For highly soluble particles with sufficiently large sizes, essentially all particles are activated into droplets, and the entire particle mass resides in the droplets (i.e., α =1).

For a column of the atmosphere of cross sectional area A and height H, the rate of loss of species S (both dissolved and interstitial) due to rainout is proportional to the rain rate (R) and the concentration of the dissolved species in the rain drops ($[S]_{dis,\ rain}$):

$$A\,H\left(\frac{\partial [S]_{tot,air}}{\partial t}\right)_{Rainout} = -\,A\,R\;\;[S]_{dis,rain} \tag{4}$$

Assuming the concentration of dissolved species in the cloud droplets is the same as that in the rain drops (i.e., $[S]_{dis,\ rain} \sim [S]_{dis,\ cloud}$), combining equations (2)–(4) yields the parameterized first-order loss rate of species S due to rainout (Garrett et al., 2006; Junge & Gustafson, 1957; Kasibhatla et al., 1991; Rehfeld & Heimann, 1995):

$$\left(\frac{\partial [S]_{totair}}{\partial t}\right)_{Rainaut} = -\frac{\alpha \rho_w R}{HLWC}[S]_{totair} = -\lambda [S]_{totair} \tag{5}$$

where λ (time^{-1}) is the loss frequency of species S, which in turn is the inverse of the rainout lifetime of species S (Giorgi & Chameides, 1986): $\tau = \lambda^{-1}$. For the sake of compactness, the subscripts are henceforth dropped, and all concentrations refer to air-equivalent concentrations of dissolved plus interstitial species. It is cautioned that the assumption that $[S]_{dis,\ rain} \sim [S]_{dis,\ cloud}$ is not entirely valid and could overestimate the effect of rainout in equation (5). Since cloud droplet composition varies across droplets size (Collett et al., 1994) and the conversion of cloud water to rain water is dependent on droplet size (Pruppacher & Klett, 1997), rain water is biased to represent the composition of the larger (more diluted) cloud droplets. This was confirmed by Fowler et al. (1988) and Kins et al. (1988), who reported that ionic concentration is greater in cloud water than in rain water, varying between a factor of 1.5 to 8.

Field data have been used to quantify the parameter α for different species. For example, in a study of stratiform clouds in the eastern United States, Daum et al. (1984) reported values between 0.6 and 0.7 for both NO_3^- and SO_4^{2-}. Collett et al. (2008) reported a value of 0.84 for total fine particle carbon for California radiation fogs. Gilardoni et al. (2014) reported values of 0.68 for ammonium and 0.5 for organics in Po Valley fog (Italy). As interstitial aerosol composition was not measured either inside or outside of clouds in the field campaigns to be addressed here, a cannot be quantified on the basis of in situ data.

Unlike α, the parameters necessary to evaluate $(\partial [S]/\partial t)_{\ Rainout}$ (mass$_{solute}$ volume$_{air}^{-1}$ time^{-1}) in equation (5) have not been characterized before (to our knowledge) in their entirety with in situ data. Rather, many studies have used a combination of meteorological field data or simulation data (for R and LWC), together with rain water composition (for $[S]$) measured off-line after collection via surface-based gauges. These studies have compared modeling results to rain water concentrations of radioactive isotopes (e.g., Brost et al., 1991;

Giorgi & Chameides, 1986; Rehfeld & Heimann, 1995; Sakashita et al., 2002) and water-soluble ions (e.g., Junge & Gustafson, 1957; Kajino & Aikawa, 2015). With respect to the column height affected by rainout, modeling studies have analyzed the troposphere (e.g., Kasibhatla et al., 1991; Neu & Prather, 2012) and the boundary layer (e.g., Russell et al., 1994). The combination of vertically resolved cloud water chemical composition, R, and LWC in the current field data set allows us to analyze the rate of removal of species due to rainout within a cloud. In section 4.2, we analyze in-cloud vertical profiles of various rainout parameters by dividing the cloud into thirds, and setting H in equation (5) equal to one third of the cloud depth. Of the 11 individual profiles obtained with the case study approach, only four have chemical composition data in each vertical third of the cloud.

4. Results and Discussion

4.1. Vertical Profiles of Species Concentrations

We hypothesize that chemical species in the marine boundary layer can be categorized into one of three different types of idealized in-cloud vertical air-equivalent concentration profiles. The following discussion applies to stratocumulus clouds as more convective clouds can additionally be impacted by entrainment from the sides. The shapes of these profiles depend on the predominant direction from which species are fed into the cloud (i.e., up through base, down from top) and the chemical reactivity of the species within cloud droplets, which in turn depends on factors such as the pH, LWC, and availability of chemical reactants. As conceptually illustrated in Figure 2, the first profile exhibits a decline of concentration with altitude in cloud for species that are unreactive and directly emitted, with a greater flux into clouds from the base rather than the top. The second profile exhibits the highest concentration somewhere in the middle of cloud for species that are reactive with a greater flux from the base of clouds; however, it is also possible that these species may enter through cloud top and the relative influence of the two vertical directions depends on a host of factors such as the species and the thermodynamic structure of the lower troposphere. The vertical location of the concentration peak likely depends on the ease with which a species enters and/or forms in a droplet (e.g., species that are formed quickly will peak closer to the base of the cloud). The last profile exhibits an increase in concentration with altitude for species with a greater flux into clouds from the top via entrainment in comparison from cloud base and/or whose photochemical production is enhanced with characteristics more favorable near cloud top (i.e., more solar irradiation).

We plot the in-cloud vertical profiles of eight species using both the case study approach and the cumulative approach and analyze how closely they resemble the idealized profiles we propose. For both approaches, the cloud depth is divided into five equally spaced vertical bins. The representative profile obtained with either approach is sensitive to whether means or medians are used. This sensitivity is due to (i) the uneven sampling of cloud water in each of the five vertical bins, and (ii) the large range in concentrations among samples in a given bin (which in some cases extends over 1 order of magnitude). Despite the significant differences between the case study approach (that uses 45 cloud water samples, each of which was collected in thin layers throughout 11 different cloud cases) versus the cumulative approach (that uses 385 cloud water samples, some of which were collected in

thick layers sometimes spanning the whole cloud depth), both approaches yield similar vertical profiles for individual species that fall into the three idealized profiles we propose.

4.1.1. Cumulative Approach—The vertical profiles of air-equivalent concentration of selected species using the cumulative approach are presented in Figure 3. The mechanisms that introduce these species into the cloud droplets are both physical (either by nucleating new droplets or by incorporating particles and gases into existing droplets) and chemical (i.e., secondary production within droplets). Three characteristic profiles emerge that match those in Figure 2. Plausible speculations are provided for why individual species adhere to a specific profile type. Speculations regarding wet scavenging are justified in section 4.4.

The first type of profile is for species without gaseous precursors that are directly emitted from the ocean surface. Sea-salt emissions from the ocean surface result in Cl^- and Na^+ concentrations being highest and lowest at cloud base and top, respectively. Their air-equivalent concentrations decrease with height owing to wet scavenging of sea salt. An additional sink is Cl^- depletion, the loss of Cl^- to the gas phase due to reactions with acids, namely, $NaCl + HA \rightarrow NaA + HCl_{(g)}$, where A denotes a conjugated base (Martens et al., 1973). As marker sizes for Cl^- are proportional to the Cl^-:Na^+ mass ratio in Figure 3, it is evident that ratios are lowest near cloud base (1.72) and increase steadily to 1.86 at cloud top; for reference, the ratio characteristic of pure sea water is 1.81. The increase of Cl^-:Na^+ mass ratio with height is statistically significant (according to a two-tailed t test: correlation coefficient (r) = 0.91;p = 0.03) and perhaps suggests that the acids (e.g., nitric, sulfuric, and organic acids) depleting Cl^- in clouds derive mainly from surface emissions rather than the free troposphere (Braun et al., 2017), thus explaining the reduction in the Cl^-:Na^+ ratio while approaching cloud base. The Cl^-:Na^+ mass ratio at cloud top is greater than the pure sea-salt ratio likely due to noise caused by using Na data from ICP-MS analysis instead of IC.

The second type of profile is for species that are produced within clouds via aqueous processing, with precursors mainly entering from cloud base but with the possibility of appreciable influences from cloud top. These species enter cloud water via either nucleation scavenging of CCN containing these species or via impaction and diffusion leading to the partitioning of precursor species into droplets, which then undergo chemical transformations. NSS SO_4^{2-}, NO_3^-, MSA, and oxalate are examples of such species. Briefly, the inorganic components NSS SO_4^{2-} and NO_3^- stem from gaseous precursors SO_2 and HNO_3 (from NO_x), respectively, that originate from anthropogenic sources in the region (e.g., shipping and continental air) and biomass burning. Ocean-emitted dimethylsulfide is the source for MSA and represents and additional pathway to produce NSS SO_4^{2-}. Oxalate is directly emitted from multiple sources (e.g., biomass burning and combustion) and is produced secondarily from volatile organic compounds via both photooxidation and aqueous chemistry in cloud droplets (e.g., Blando & Turpin, 2000; Chebbi & Carlier, 1996; Kawamura & Kaplan, 1987).

Unlike species whose sole source is surface emission of primary particles, species belonging to the second type of profile do not exhibit the highest concentration at cloud base. Rather, their concentrations do not decline immediately above cloud base and they exhibit a

maximum somewhere in the middle of the cloud, before declining in concentration near cloud top; this is due to species of the second type of profile having an in-cloud source. The data set does not allow for determining the relative strength of the flux from the cloud base or from cloud top for NSS SO_4^{2-}, NO_3^-, MSA, and oxalate; as these species have documented sources from the ocean surface and ship exhaust, it is presumed that their main route of entry is from cloud base; however, this certainly does not preclude the possibility of them entering from cloud top via entrainment of free tropospheric gases and aerosol. To emphasize the latter point, past work in the study region has shown that thin layers of aerosol exist above stratocumulus cloud tops enriched with oxalate and MSA (Sorooshian et al., 2007), which could entrain into clouds and impact droplet composition. It should also be noted that it is possible that some species that require longer times for production (e.g., some organics may need more time than sulfate or nitrate) could potentially be produced more near cloud top; conversely, species requiring very small amounts of time could be produced more near cloud base. Thus, the explanation for the second type of profile requires caution with regard to the time scale of production for a species. In other words, the location of the peak in concentration of a species depends on the characteristic time scale necessary to produce that species; the variation in the peak location is shown as the shaded area in Figure 2.

The third type of profile is representative of species that enter mainly from cloud top rather than cloud base and/or can also be produced photochemically near cloud top. Formate and NO_2^- fit into this category. Formate stems from direct emissions from a variety of sources (e.g., plants and soils) in addition to being secondarily produced in the gas phase via oxidation of volatile organic compounds emitted from combustion and biogenic sources (Keene et al., 1995; Stavrakou et al., 2012; Talbot et al., 1995). Formate is also produced in the aqueous phase via hydroxyl radical (OH) oxidation of organic species such as hydrated formaldehyde (Chameides & Davis, 1983) and tryptophan (Bianco et al., 2016). Nitrite measurements in clouds are scarce due to its low concentrations and its fast oxidation (Acker et al., 2008), but it has been linked to continental emissions (Wang et al., 2014) and heterogeneous reactions of NO_2 in clouds (Lammel & Metzig, 1998). Air masses from continental emissions can enter the free troposphere and be transported long distances. Once over the marine boundary layer, continentally influenced air masses can enter the cloud deck in the study region via entrainment (Coggon et al., 2014). As will be expanded upon in section 4.1.3, other factors may lead to higher concentrations near cloud top other than entrainment, including factors associated with chemical reactivity, pH, and solar irradiance.

There was considerable variability in each vertical bin for the species concentrations shown. The horizontal whiskers represent 10% of the standard deviation rather than the full value to be able to more easily display the vertical variability of the mean values. At least three reasons for the high variability include (i) samples being influenced by different sources, (ii) single cloud water samples having been collected over multiple vertical bins rather than a single bin, and (iii) varying numbers of points used for the calculations in each of the five vertical bins (shown in Figure 3 next to the error bars). It can be argued that the large standard deviation of the cumulative approach discredits the validity of any trends observed in the vertical profiles. However, the same trends emerge when using a more rigorous approach that is discussed in the next section.

4.1.2. Case Study Approach—The 11 individual profiles obtained using the case study approach of each of the eight selected species are shown in Figures S2–S9. In this section, we take the mean of those 11 profiles for each species in order to find general representative profiles for comparison with profiles obtained using the cumulative approach.

Both the case study approach and the cumulative approach present the disadvantages of (i) having uneven coverage of cloud water in each cloud bin and (ii) having a large range of measurements in each bin caused by sampling different air masses. The consequences of these disadvantages in calculating a representative profile are now explored. Figure 4a displays the 11 profiles of Cl^- obtained using the case study approach in gray with mean and median concentrations shown in black and red, respectively. The number of cloud water data points used in each bin is placed next to the standard deviation error bars. Concentrations of an individual species vary by up to 1 order of magnitude. To place all the profiles on a more comparable scale, each profile is divided by the average concentration of that profile (i.e., each profile is normalized); of interest is the shape of the concentration profile and not concentration values. Figure 4b shows the 11 normalized Cl^- profiles in gray with their mean and median again shown in black and red, respectively. Comparing Figures 4a and 4b demonstrates that the shape of the representative vertical profile is sensitive to the statistical method used, for example, Figure 4a shows a peak in mean concentration in the middle of cloud, whereas Figure 4b shows a peak in mean normalized concentration at cloud base. The shape of a representative profile is captured better by the mean of normalized concentrations, since the normalization process helps cancel the effect of averaging concentration values that are significantly different. The operations of normalizing, averaging, and obtaining medians do not have the same consequences for every species; for example, these operations do not affect NO_3^- (Figures 4c and 4d) in the same way as Cl^-. We believe these differences do not elucidate the nature of any physical or chemical phenomena, rather, they are due to the uneven amount of measurements distributed along the cloud depth.

Figure 5 reports the results using the normalization approach from Figures 4b and 4d for the eight selected species. With the exception of formate, the vertical profiles resemble the main features already described in Figure 3. Formate had fewer data points than all other species using the case study approach (see Figure S9), which may have contributed to its different behavior in Figure 5 versus Figure 3. As is observed in the cumulative approach, the Cl^-:Na^+ ratio also increases with cloud height (1.66 at base and 2.17 at top) and the increase is again statistically significant ($r = 0.90$; $p = 0.04$). The normalization approach unfortunately cannot be conducted for Figure 3 as those data included flights where maybe only one sample was collected in a cloud representing either one or all parts of a cloud. The mean normalized profiles obtained using the case study approach (Figure 5) and the profiles obtained using the cumulative approach (Figure 3) resemble the idealized profiles we propose in Figure 2. However, some individual profiles collected using the case study approach (Figures S2-S9) differ substantially from the profiles in Figures 2, 3, and 5. Section 4.3 examines the potential role of rainout in leading to these conflicting results by analyzing relationships between vertical in-cloud profiles of R and species concentrations.

The 11 “case study” profiles were also used to analyze each of the eight species and examine the possibility of cloud water concentration being dependent on cloud base height. For example, precursor species (e.g., SO_2 in the case of NSS SO_4^{2-}) could be depleted to a greater extent before reaching higher cloud base heights. No statistically significant correlation was found for any species when comparing the cloud-mean air-equivalent concentration versus cloud base height (Table S2). Though this finding might be a shortcoming of the limited amount of data points, it also could point to insignificant reactivity of the measured species (and associated precursors) during their transport from the ocean surface to cloud base.

4.1.3. Dependence of Vertical Profiles on LWC, pH, and Availability of Chemical Reactants—

It must be emphasized that the profiles for each species we propose in Figure 2 (and observe in Figures 3 and 5) are neither fixed nor permanent; the profiles of each species certainly change with the conditions of the environment. As has already been suggested, the chemical reactivity of a species in droplets has an influence on the vertical profile of concentration and, in turn, the chemical reactivity of species in clouds is highly dependent on numerous factors such as LWC, pH, and the availability of chemical reactants; these factors are briefly discussed in this section using formate as an example.

Consider the simplified scenario of formic acid gas that partitions into cloud droplets: (i) the fraction of formic acid that is partitioned into the aqueous phase depends on LWC and Henry’s law constant, (ii) the fraction of formic acid that subsequently dissociates into formate ions depends on the pH of the solution, and (iii) the reaction pathway the formate ion undergoes is highly sensitive to the solution pH and the chemical reactants available in the droplet (Keene & Galloway, 1986; Munger et al., 1989b; Schwartz, 1986; Seinfeld & Pandis, 2016). Simultaneously, formate can also be formed in the droplet by oxidation of precursor organic species; the OH radical serves as both a source and sink for formate and can be either scavenged from the gas phase or photo-generated in the aqueous phase (Chameides & Davis, 1983) (e.g., NO_3^-, NO_2^-, and iron complexes serve as sources of photo-generated OH radicals; Bianco et al., 2015).

We chose formate for this discussion because it serves as an example that physical and chemical effects can be superimposed on each other to modify vertical concentration profiles. We hypothesize that the significant peak in formate air-equivalent concentration in Figure 3 is the result of superimposing a physical effect and a chemical effect. The physical effect is the potential entrainment of formate (coming from continental sources) form in the free troposphere into the cloud top; the chemical effect is the formation of formate at cloud top due to factors associated with potentially enhanced pH and photochemistry. Since formate is produced by the OH-mediated oxidation of organic substances like tryptophan (Bianco et al., 2016), and OH is photogenerated, it is reasonable that a greater solar irradiance at cloud top should produce more OH and cause a peak in formate concentration. Perhaps this peak is diminished at nighttime, leaving only the physical entrainment effect to be observed.

It is interesting to note that the pH conditions throughout the cloud depth are sufficiently high so as to permit most of the formic acid to dissociate into formate; this occurs when pH

> 4 (Seinfeld & Pandis, 2016). The vertical profile of pH obtained using the case study approach is shown in Figure S10. Throughout the cloud, pH always exceeded 4; therefore, most of the formic acid dissociated into formate. Consistent with the trend reported by Leaitch et al. (1983), pH increases with cloud height (the increase is statistically significant: $r = 0.90$; $p = 0.03$). Most of the individual pH profiles (Figure S11) exhibit an increase of pH with height.

4.2. Vertical Profiles of Rainout Parameters

In order to study the effect of rainout on in-cloud vertical concentration profiles, it is convenient to analyze species with both minimal chemical reactivity in cloud droplets and a relatively constant flux over the sampled area. Of the species shown in Figures 3 and 5, Cl^- and Na^+ best satisfy these constraints and are examined in greater detail here. This section probes the four profiles that contain chemical data in all thirds of the cloud by focusing on how cloud conditions (R, LWC, and H) affect the rate of rainout and chemical composition, and in section 4.3 an alternative approach is used to make use of all 11 profiles by relating cloud conditions to chemical composition.

The four profiles with chemical data in each third of clouds are from E-PEACE RFs 10,18, and 24, and NiCE RF11. Figure 6 summarizes the cloud depths (212–488 m) and base heights (162–236 m) for the four cases, in addition to vertical profiles of the air-equivalent mass concentration of Cl^- and Na^+, R, LWC, λ (equation (5)), τd, and the loss rate of Cl^- and Na^+ concentration due to rainout ($(\partial[Cl^-]/\partial t)_{Rainout}$ and $\left(\partial\left[Na^+\right]/\partial t\right)_{Rainout}$; equation (5)).

Since sea-salt particles are large and highly hygroscopic, it is assumed that a for both Cl^- and Na^+ is unity; consequently, λ and τ depend exclusively on R, LWC, and H. Vertical profiles of Cl^- are parallel to those of Na^+ (Figure 6a), which is expected since both species are transported together as sea salt. Comparing Figures 6b and 6c shows that even though LWC and R are related through the collision-coalescence process, they vary independently of one another (e.g., E-PEACE RF10 and NiCE RF11 have the same LWC profile but have different R profiles).

To explain how R profiles could affect concentration profiles, consider two consecutive vertical layers within a cloud, with the highest layer exhibiting a greater R. Both interstitial and dissolved species can be transported upward (from the lower to the higher layer) due to updrafts, turbulent diffusion, and other mechanisms. When the small upward-moving particles and cloud droplets encounter large downward-moving rain drops, some particles and droplets can be intercepted, impeding their entrance into the higher layer. In addition, the species dissolved in the large rain drops are being removed from the highest layer, which will further reduce the concentration in the highest layer. Consistent with this concept is the observation from Figures 6a and 6b that when R increases (decreases) from one layer to the next above it, concentrations of Cl^- and Na^+ decrease (increase). An exception to this is E-PEACE RF18, which exhibited the lowest R in the top third of the cloud among all four cases, suggesting that identifying a relationship between R and concentration profiles could require a threshold value of R near cloud top. At low magnitudes of R, other mechanisms (such as turbulent diffusion) could play a more significant role in governing the concentration profile. More flight data are required to support this claim.

Figures 6d and 6e show that for three of the four cases, λ is greatest (and τ is lowest) in the bottom third of the cloud, indicating that rainout is most efficient in the bottom third of the clouds since species dissolved in droplets are removed the fastest and spend the least amount of time there. Values of λ and τ range between 4.35×10^{-5}–1.82×10^{-3} s^{-1} and 5.50×10^{2}–2.30×10^{4} s, respectively. Giorgi and Chameides (1986) suggested that τ for a soluble species at a given altitude depends on (i) the solubility of the species (represented here as α), (ii) the direction of the species' flow (i.e., from above or below the altitude of interest), and (iii) the precipitation regime (i.e., amount, duration, and frequency of precipitation). The effect of precipitation regime on τ is clearest for NiCE RF11. Three features distinguish it from the other profiles: (i) it presents the lowest R of all profiles in the bottom third of the cloud, (ii) its R profile is significantly different than the rest by presenting a pronounced increase with altitude in cloud, and (iii) it is the thinnest of the four clouds considered. These factors suggest that the cloud was not sufficiently thick to produce drizzle, in which case the vertical profile of drop size distribution is determined primarily by condensational growth leading to larger droplet diameters and LWC in the top third of the cloud (Wood, 2005). Even though these characteristics are not entirely descriptive of the lifestage (i.e., young or old) of a cloud, NiCE RF11 might have been in its incipient stages as compared to the other cases. Comparison of the four cases demonstrates the importance of the precipitation regime in driving the efficiency of rainout within a cloud, as quantified by λ or τ.

With the exception of NiCE RF11, $(\partial[\mathrm{Cl}^-]/\partial t)_{\mathrm{Rainout}}$ and $\left(\partial\left[\mathrm{Na}^+\right]/\partial t\right)_{\mathrm{Rainout}}$ are greatest at cloud base (Figure 6f). Ranges of Cl^- and Na^+ losses due to rainout for the four cases are 2.85×10^{-5}–6.81×10^{-3} μg m^{-3} s^{-1} and 1.45×10^{-5}–3.23×10^{-3} μg m^{-3} s^{-1}, respectively. Comparing Figures 6a and 6e raises an important question: Why does the bottom third of the cloud usually exhibit the greatest loss due to rainout and also the greatest concentration? In part, this is a consequence of $(\partial[S]/\partial t)_{\mathrm{Rainout}}$ being proportional to $[S]$, via equation (5).

More importantly, this is a consequence of updrafts carrying sea-salt particles into the bottom third of the cloud. These particles would activate into new droplets, thus increasing the air-equivalent concentration of Cl^- and Na^+ and largely offsetting the decrease in concentration due to rainout.

4.3. Ratios of Rainout Lifetimes and Concentrations

In order to take advantage of all 11 profiles in the case study approach, a different analysis was applied that does not require cloud water measurements in each third of clouds. This analysis consists of comparing cloud layer pairs: bottom/top (B/T), middle/top (M/T), and bottom/middle (B/M). As shown already, a layer with higher R will generally have a lower air-equivalent species concentration in the absence of an in-cloud production mechanism. Here we analyze τ instead of R as τ is more directly related to rainout; the more time a species spends in a layer (i.e., higher τ), the greater its concentration will be in that layer. Figure 7 shows the ratio of lower-to-higher altitude air-equivalent concentration for Cl^- and Na^+ plotted against the ratio of lower-to-higher altitude τ for the three aforementioned layer pairs. Notice that even though altitude within a cloud affects LWC and cloud droplet size, which in turn affects droplet chemistry (Bator & Collett, 1997) and diffusion and impaction of species into droplets (Seinfeld & Pandis, 2016), if α is assumed to be constant fora

species along the depth of the cloud, then the ratio of t between two layers becomes insensitive to α. The assumption of constant α consequently introduces noise into the analysis.

We interpret the slope of the linear regression equations shown as indicative of rainout strength and interpret the r as the degree to which rainout governs the vertical concentration profiles for a species. The objective of the subsequent analysis is to investigate how rainout affects the profiles shown in Figures 3 and 5. The correlational method presented here helps support two theories proposed in this study: (i) vertical concentrations of unreactive surface-derived species are very sensitive to rainout and (ii) rainout is most efficient in the bottom two thirds of the cloud. A cluster of data exists where the x axis (τ ratios) values are <1; this is because τ is inversely proportional to R, which for precipitating clouds is typically greatest in the bottom third of clouds (Wood, 2005).

The following characteristics are evident from Figure 7: (i) the high correlation coefficients for Na^+ ($r = 0.98$; $p < 0.01$) and Cl^- ($r = 0.99$; $p < 0.01$) when comparing the B/T thirds of the cloud suggest that rainout significantly influences their vertical profiles; (ii) the similar B/T slopes for Na^+ and Cl^- (0.36–0.42) are consistent with a common source for the two species (i.e., sea salt); (iii) the higher slopes for Na^+ and Cl^- (0.99–1.16) when comparing B/M versus B/T indicates that rainout strength is higher in the bottom two thirds of clouds, as is clear from observing vertical concentration gradients in the individual profiles (Figures S2 and S3); and (iv) the correlations when analyzing the M/T thirds are insignificant because of reduced material at cloud top available for scavenging.

Table 2 summarizes the linear regression coefficients for all the species shown in Figures 3 and 5, in addition to elemental iron (Fe). Differences in B/T and B/M slopes and correlations between the other species and sea salt most likely are due to factors other than precipitation that govern their vertical profiles, such as formation or depletion reactions and cloud top entrainment. NSS SO_4^{2-}, NO_3^-, MSA, and oxalate exhibited B/T slopes between 0.21 and 0.31, which are less than sea-salt constituents likely because the latter do not have a production mechanism inside clouds. MSA and oxalate exhibited reduced rainout strength for B/M (slopes of 0.61 and 0.76, respectively) as compared to Na^+, Cl^-, NSS SO_4^{2-}, and NO_3^- (0.99–1.16). A potential explanation is that MSA and oxalate require time to be produced in cloud and their concentrations can increase with altitude above cloud base. Another possible explanation is that MSA and oxalate are mainly contained in small droplets, which are converted less efficiently to rain drops, which ultimately are removed by rainout. Therefore, MSA and oxalate are less affected by rainout.

Compared to the other aforementioned species, oxalate exhibited reduced correlations for B/T ($r = 0.38$; $p = 0.53$) and B/M ($r = 0.35$; $p = 0.56$). A plausible explanation is an additional sink via iron-complexation, which has been reported for clouds in the study region (Sorooshian, Wang, Coggon, et al., 2013). Multiple individual profiles for Fe and oxalate exhibit opposite vertical trends with reduced Fe levels when oxalate is enhanced, and vice versa (Figures S7 and S12). Fe exhibits a B/M slope of 1.22 and a fairly high correlation ($r = 0.75$; $p = 0.09$), similar to other species that lack a secondary source or a depletion mechanism in clouds.

Owing to past work in the study region linking enhanced NO_2^- levels to continental emissions that entrain in clouds at their top, it is expected that NO_2^- would exhibit the lowest B/T and B/M slopes, which is the case (0.13 and 0.27, respectively). NO_2^- also exhibited the lowest correlation for B/M ($r = 0.28$;$p = 0.59$) as there is less rainout potential in the bottom two thirds of clouds owing to its highest levels being at cloud top. While formate exhibited positive slopes for the B/T and B/M categories (0.18 and 0.42, respectively), formate had less data availability and had the second lowest correlations among Table 2 species.

The nonzero y-intercepts of the regression equations in Table 2 have significance. In the hypothetical case that x equals zero in the regression equations for B/M, caused by a large R in the lowest layer (i.e., τ in the lowest layer approaches zero), Cl^- and Na^+ concentrations in the lowest layer are not zero. This is presumably a result of the replenishment of sea salt due to nucleation scavenging of particles in updrafts near cloud base. The y-intercepts of the B/T regression equations are less meaningful as an extra vertical layer interferes with the signature of nucleation scavenging at cloud base. Nucleated droplets at cloud base may be removed before reaching the middle third of clouds, which also leads to the y-intercepts of the M/T regressions being less meaningful.

4.4. Implications for Modeling

The results of this study have implications for improving the treatment of wet scavenging processes in both climate models and process-oriented models. In the case of the CAM5 model, there are seven layers below 1.2 km, with the layer thickness varying between 100 and 250 m; thus, while this model can potentially have three layers for the types of marine boundary layer clouds examined here, global models with higher vertical resolution will have a better chance. Wang et al. (2013) found that the global spatial distribution of particles in CAM5 is very sensitive to the uncertain parameters associated with the model's wet scavenging scheme. Those parameters are usually calibrated by evaluating the long-term mean aerosol properties against observations over a regional domain and then applied to the same type of clouds (i.e., stratiform or convective clouds) uniformly. The results of this work motivate consideration of the lifestage of clouds for climate models simulating wet scavenging. As shown in section 4.2, the vertical profile of λ within stratocumulus clouds depends on the characteristics of precipitation, which could be related to cloud lifestage. However, it is often quite challenging for climate models to correctly simulate the vertical profiles of LWC and R that are used to characterize the loss frequency λ at small scales. The relationships shown in Figure 7, which have less dependence on LWC and R, are more practical for climate model evaluation, since climate models do not necessarily provide accurate estimates of the magnitudes of LWC or R, but rather they can calculate their ratios correctly. Process models such as the Weather Research and Forecasting model coupled with Chemistry (WRF-Chem) (Kazil et al., 2011) running at fine spatial and temporal resolutions can better resolve clouds and precipitation and represent the detailed aerosol chemical, microphysical, and transport processes. They can be directly evaluated against the observational results here and used to bridge the gap between small-scale field measurements and climate models.

Rainout is only one of the many physical and chemical mechanisms influencing vertical profiles of cloud water species concentrations. Future work is warranted to analyze the relative contribution of rainout relative to several other mechanisms such as the following: (i) formation of new droplets via nucleation scavenging; (ii) incorporation of gases and interstitial particles into existing droplets via impaction and Brownian diffusion; (iii) evaporation of droplets such as with dry air entrainment; (iv) transport and mixing of droplets due to turbulent diffusion, advection, and convection; and (v) loss of Cl^- (in the form of HCl) to the gas phase due to reactions with acids.

It is important to note that this study focused on warm marine stratocumulus clouds and the findings are not necessarily applicable to other cloud systems. For example, in warm clouds, a droplet's solute remains in the liquid phase as cloud water is converted to rain water; whereas in mixed-phase clouds, via the Bergeron process, the solute is released back into the atmosphere when droplets evaporate and the resulting evaporated water deposits onto ice crystals thus making the ice crystals grow (Barrie, 1985). In addition, the ion concentration in precipitation exiting mixed-phase clouds is affected by the riming process (the capture of super-cooled cloud droplets by snow crystals), a process that does not exist in warm clouds (Collett et al., 1991). More research is necessary to determine if the idealized profiles we propose are also valid in other cloud systems.

5. Conclusions

Cloud water samples collected from stratocumulus clouds off the California coast are used to construct vertical profiles of air-equivalent concentrations of major water-soluble species. The effect of the rainout component of wet scavenging on these profiles was examined. The main findings include the following:

1. Three characteristic species concentration profiles were identified: (i) species peaking in concentration at cloud base with an overall reduction in concentration with altitude due to entering cloud base via updrafts and a lack of in-cloud production mechanisms (e.g., Cl^- and Na^+); (ii) species with an overall increase in concentration with altitude with concentration peaking at cloud top owing to some combination of tropospheric sources that enter the cloud top via entrainment and chemical factors such as photochemically induced reactions, lengthier time to be produced if introduced from cloud base, and pH-dependent processes (e.g., formate and NO_2^-); and (iii) species peaking in concentration in the middle of clouds due to secondary production within droplets (e.g., NSS SO_4^{2-}, NO_3^-, and organic acids).
2. The vertical profiles of rainout loss frequency (λ) and rainout lifetime (τ) are dependent on the precipitation regime, potentially related to the cloud's lifestage. Thin clouds with light drizzle rates exhibit a greater A at cloud top, whereas thick clouds with moderate drizzle rates have a greater λ at cloud base.
3. Whereas the loss rate of species due to rainout is greatest in the bottom third of clouds, such species concentrations are also highest in the bottom layer. This shows the importance of modeling updrafts carrying CCN (and thus, nucleation

scavenging of these particles) in order to correctly represent the replenishment of surface-derived particles.

4. Vertical profiles of surface-derived species (Cl^- and Na^+) are those mostly influenced by rainout, while those with free tropospheric sources and in-cloud formation mechanisms are less influenced.

Supplementary Material

Refer to Web version on PubMed Central for supplementary material.

Acknowledgments

All data used in this work can be found in the Figshare database (Sorooshian et al., 2017). This work was funded by Office of Naval Research grants N00014–10-1–0811, N00014–11-1–0783, N00014–10-1–0200, N00014–04-1–0118, and N00014–16-1–2567. A. MacDonald acknowledges support from the Mexican National Council for Science and Technology (CONACyT). H. Wang acknowledges support from the United States Department of Energy (DOE) Office of Science, Biological and Environmental Research. The Pacific Northwest National Laboratory (PNNL) is operated for DOE by Battelle Memorial Institute under contract DE-AC05–76RLO1830. The authors gratefully acknowledge Jan Kazil for useful discussions.

References

Acker K, Beysens D, & Möller D (2008). Nitrite in dew, fog, cloud and rain water: An indicator for heterogeneous processes on surfaces. Atmospheric Research, 87(3–4), 200–212. https://doi.org/10.10167j.atmosres.2007.11.002

Barrie LA (1985). Scavenging ratios, wet deposition, and in-cloud oxidation: An application to the oxides of Sulphur and nitrogen. Journal of Geophysical Research, 90(D3), 5789–5799. 10.1029/JD090iD03p05789

Barth MC, Rasch PJ, Kiehl JT, Benkovitz CM, & Schwartz SE (2000). Sulfur chemistry in the National Center for Atmospheric Research Community Climate Model: Description, evaluation, features, and sensitivity to aqueous chemistry. Journal of Geophysical Research, 105(D1), 1387–1415. 10.1029/1999JD900773

Bator A, & Collett JL (1997). Cloud chemistry varies with drop size. Journal of Geophysical Research, 102(D23), 28,071–28,078. 10.1029/97JD02306

Benedict KB, Lee T, & Collett JL (2012). Cloud water composition over the southeastern Pacific Ocean during the VOCALS regional experiment. Atmospheric Environment, 46, 104–114. https://doi.org/10.1016Zj.atmosenv.2011.10.029

Bianco A, Passananti M, Perroux H, Voyard G, Mouchel-Vallon C, Chaumerliac N, et al. (2015).A better understanding of hydroxyl radical photochemical sources in cloud waters collected at the puy de Dôme station—Experimental versus modelled formation rates. Atmospheric Chemistry and Physics, 15(16), 9191–9202. 10.5194/acp-15-9191-2015

Bianco A, Passananti M, Deguillaume L, Mailhot G, & Brigante M (2016). Tryptophan and tryptophan-like substances in cloud water: Occurrence and photochemical fate. Atmospheric Environment, 137, 53–61. 10.1016/j.atmosenv.2016.04.034

Blando JD, & Turpin BJ (2000). Secondary organic aerosol formation in cloud and fog droplets: A literature evaluation of plausibility. Atmospheric Environment, 34(10), 1623–1632. 10.1016/S1352-2310(99)00392-1

Boone EJ, Laskin A, Laskin J, Wirth C, Shepson PB, Stirm BH, & Pratt KA (2015). Aqueous processing of atmospheric organic particles in cloud water collected via aircraft sampling. Environmental Science & Technology, 49(14), 8523–8530. 10.1021/acs.est.5b01639

Braun RA, Dadashazar H, MacDonald AB, Aldhaif AM, Maudlin LC, Crosbie E, et al. (2017). Impact of wildfire emissions on chloride and bromide depletion in marine aerosol particles. Environmental Science & Technology, 51(16), 9013–9021. 10.1021/acs.est.7b02039 [PubMed: 28700243]

Brost RA, Feichter J, &Heimann M (1991). Three-dimensional simulation of Be in a global climate model. Journal of Geophysical Research, 96(D12), 22,423–22,445. 10.1029/91JD02283

Chameides WL, & Davis DD (1983). Aqueous-phase source of formic acid in clouds. Nature, 304(5925), 427–429. 10.1038/304427a0

Chebbi A, & Carlier P (1996). Carboxylic acids in the troposphere, occurrence, sources, and sinks: A review. Atmospheric Environment, 30(24), 4233–4249. 10.1016/1352-2310(96)00102-1

Chen YC, Christensen MW, Xue L, Sorooshian A, Stephens GL, Rasmussen RM, & Seinfeld JH (2012). Occurrence of lower cloud albedo in ship tracks. Atmospheric Chemistry and Physics, 12(17), 8223–8235. 10.5194/acp-12-8223-2012

Cini R, Prodi F, Santachiara G, Porcu F, Bellandi S, Stortini AM, et al. (2002). Chemical characterization of cloud episodes ata ridge site in Tuscan Appennines, Italy. Atmospheric Research, 61(4), 311–334. 10.1016/S0169-8095(01)00139-9

Coggon MM, Sorooshian A, Wang Z, Craven JS, Metcalf AR, Lin JJ, et al. (2014). Observations of continental biogenic impacts on marine aerosol and clouds off the coast of California. Journal of Geophysical Research: Atmospheres, 119, 6724–6748. 10.1002/2013JD021228

Collett JL, Prevot ASH, Staehelin J, & Waldvogel A (1991). Physical factors influencing winter precipitation chemistry. Environmental Science & Technology, 25(4), 782–788. 10.1021/es00016a025

Collett JL, Bator A, Rao X, & Demoz BB (1994). Acidity variations across the cloud drop size spectrum and their influence on rates of atmospheric sulfate production. Geophysical Research Letters, 21(22), 2393–2396. 10.1029/94GL02480

Collett JL, Herckes P, Youngster S, & Lee T (2008). Processing of atmospheric organic matter by California radiation fogs. Atmospheric Research, 87(3–4), 232–241. 10.1016/j.atmosres.2007.11.005

Crahan KK, Hegg D, Covert DS, & Jonsson H (2004). An exploration of aqueous oxalic acid production in the coastal marine atmosphere. Atmospheric Environment, 38(23), 3757–3764. https://doi.org/10.1016Zj.atmosenv.2004.04.009

Crosbie E, Wang Z, Sorooshian A, Chuang PY, Craven JS, Coggon MM, et al. (2016). Stratocumulus cloud clearings and notable thermodynamic and aerosol contrasts across the clear-cloudy Interface. Journal of the Atmospheric Sciences, 73(3), 1083–1099. 10.1175/Jas-D-15-0137.1

Dadashazar H, Wang Z, Crosbie E, Brunke M, Zeng XB, Jonsson H, et al. (2017). Relationships between giant sea salt particles and clouds inferred from aircraft physicochemical data. Journal of Geophysical Research: Atmospheres, 122, 3421–3434. 10.1002/2016JD026019

Dadashazar H, Braun RA, Crosbie E, Chuang PY, Woods RK, Jonsson HH, & Sorooshian A (2018). Aerosol characteristics in the entrainment interface layer in relation to the marine boundary layer and free troposphere. Atmospheric Chemistry and Physics, 18(3), 1495–1506. 10.5194/acp-18-1495-2018

Daum PH, Kelly TJ, Schwartz SE, & Newman L (1984). Measurements of the chemical-composition of stratiform clouds. Atmospheric Environment, 18(12), 2671–2684. 10.1016/0004-6981(84)90332-9

Deininger CK, &Saxena VK (1997). A validation of back trajectories of air masses by principal component analysis of ion concentrations in cloud water. Atmospheric Environment, 31(2), 295–300. 10.1016/1352-2310(96)00152-5

Desyaterik Y, Sun Y, Shen XH, Lee TY, Wang XF, Wang T, & Collett JL (2013). Speciation of “brown” carbon in cloud water impacted by agricultural biomass burning in eastern China. Journal of Geophysical Research: Atmospheres, 7 78, 7389–7399. 10.1002/jgrd.50561

Easter RC, Ghan SJ, Zhang Y, Saylor RD, Chapman EG, Laulainen NS, et al. (2004). MIRAGE: Model description and evaluation of aerosols and trace gases. Journal of Geophysical Research, 709, D20210. 10.1029/2004JD004571

Ervens B (2015). Modeling the processing of aerosol and trace gases in clouds and fogs. Chemical Reviews, 115(10), 4157–4198. 10.1021/cr5005887 [PubMed: 25898144]

Feingold G, McComiskey A, Rosenfeld D, & Sorooshian A (2013). On the relationship between cloud contact time and precipitation susceptibility to aerosol. Journal of Geophysical Research: Atmospheres, 118, 10,544–10,554. 10.1002/jgrd.50819

Fomba KW, van Pinxteren D, Müller K, Iinuma Y, Lee T, Collett JL, & Herrmann H (2015). Trace metal characterization of aerosol particles and cloud water during HCCT 2010. Atmospheric Chemistry and Physics, 15(15), 8751–8765. 10.5194/acp-15-8751-2015

Fowler D, Cape JN, Leith ID, Choularton TW, Gay MJ, & Jones A (1988). The influence of altitude on rainfall composition at great dun fell. Atmospheric Environment, 22(7), 1355–1362. 10.1016/0004-6981(88)90160-6

Garrett TJ, Avey L, Palmer PI, Stohl A, Neuman JA, Brock CA, et al. (2006). Quantifying wet scavenging processes in aircraft observations of nitric acid and cloud condensation nuclei. Journal of Geophysical Research, 111, D23S51. 10.1029/2006JD007416

Gerber H, Arends BG, & Ackerman AS (1994). New microphysics sensor for aircraft use. Atmospheric Research, 31(14), 235–252. 10.1016/0169-8095(94)90001-9

Ghauri BM, Mirza MI, Richter R, Dutkiewicz VA, Rusheed A, Khan AR, & Husain L (2001). Composition of aerosols and cloud water at a remote mountain site (2.8 kms) in Pakistan. Chemosphere - Global Change Science, 3(1), 51–63. 10.1016/S1465-9972(00)00038-6

Gilardoni S, Massoli P, Giulianelli L, Rinaldi M, Paglione M, Pollini F, et al. (2014). Fog scavenging of organic and inorganic aerosol in the Po Valley. Atmospheric Chemistry and Physics, 14(13), 6967–6981. 10.5194/acp-14-6967-2014

Gioda A, Mayol-Bracero OL, Reyes-Rodriguez GJ, Santos-Figueroa G, & Collett JL (2008). Water-soluble organic and nitrogen levels in cloud and rainwater in a background marine environment under influence of different air masses. Journal of Atmospheric Chemistry, 67(2), 85–99. 10.1007/s10874-009-9125-6

Gioda A, Mayol-Bracero OL, Morales-García F, Collett J, Decesari S, Emblico L, et al. (2009). Chemical composition of cloud water in the Puerto Rican tropical trade wind cumuli. Water, Air, & Soil Pollution, 200(1–4), 3–14. 10.1007/s11270-008-9888-4

Gioda A, Mayol-Bracero OL, Scatena FN, Weathers KC, Mateus VL, & McDowell WH (2013). Chemical constituents in clouds and rainwater in the Puerto Rican rainforest: Potential sources and seasonal drivers. Atmospheric Environment, 68, 208–220. 10.1016/j.atmosenv.2012.11.017

Giorgi F, & Chameides WL (1986). Rainout lifetimes of highly soluble aerosols and gases as inferred from simulations with a general-circulation model. Journal of Geophysical Research, 91 (D13), 14,367–14,376. 10.1029/JD091id13p14367

Gong WM, Stroud C, & Zhang LM (2011). Cloud processing of gases and aerosols in air quality modeling. Atmosphere, 2(4), 567–616. 10.3390/atmos2040567

Gunn R, & Kinzer GD(1949). The terminal velocity of fall for water droplets ins stagnant air. Journal of Meteorology, 6(4), 243–248. 10.1175/1520-0469(1949)006<0243:TTV0FF>2.0.C0;2

Hayden KL, Macdonald AM, Gong W, Toom-Sauntry D, Anlauf KG, Leithead A, et al. (2008). Cloud processing of nitrate. Journal of Geophysical Research, 113, D18201. 10.1029/2007JD009732

Hegg DA, & Hobbs PV (1986). Studies of the mechanisms and rate with which nitrogen species are incorporated into cloud water and precipitation, Second Annual Report on Project CAPA-21–80 to the Coordinating Research Council.

Hegg DA, Gao S, & Jonsson H (2002). Measurements of selected dicarboxylic acids in marine cloud water. Atmospheric Research, 62(1–2), 1–10. 10.1016/S0169-8095(02)00023-6

Hutchings JW, Robinson MS, McIlwraith H, Triplett Kingston J, & Herckes P (2008). The chemistry of intercepted clouds in Northern Arizona during the North American monsoon season. Water, Air, and Soil Pollution, 199(1–4), 191–202. 10.1007/s11270-008-9871-0

Junge CE, & Gustafson PE (1957). On the distribution of sea salt over the United States and its removal by precipitation. Tellus, 9(2), 164–173. 10.3402/tellusa.v9i2.9092

Kajino M, & Aikawa M (2015). A model validation study of the washout/rainout contribution of sulfate and nitrate in wet deposition compared with precipitation chemistry data in Japan. Atmospheric Environment, 117,124–134. https://doi.org/10.1016Zj.atmosenv.2015.06.042

Kasibhatla PS, Levy H, Moxim WJ, & Chameides WL (1991). The relative impact of stratospheric photochemical production on tropospheric NO_y levels: A model study. Journal of Geophysical Research, 96(D10), 18,631–18,646. 10.1029/91JD01665

Kawamura K, & Kaplan IR (1987). Motor exhaust emissions as a primary source for dicarboxylic-acids in Los-Angeles ambient air. Environmental Science & Technology, 21 (1), 105–110. 10.1021/es00155a014

Kazil J, Wang H, Feingold G, Clarke AD, Snider JR, & Bandy AR (2011). Modeling chemical and aerosol processes in the transition from closed to open cells during VOCALS-REx. Atmospheric Chemistry and Physics, 11(15), 7491–7514. 10.5194/acp-11-7491-2011

Keene WC, & Galloway JN (1986). Considerations regarding sources for formic and acetic-acids in the troposphere. Journal of Geophysical Research, 91(D13), 14,466–14,474. 10.1029/JD091iD13p14466

Keene WC, Mosher BW, Jacob DJ, Munger JW, Talbot RW, Artz RS, et al. (1995). Carboxylic-acids in clouds at a high-elevation forested site in Central Virginia. Journal of Geophysical Research, 100(D5), 9345–9357. 10.1029/94JD01247

Kins L, Müller KP, Ehhalt DH, & Meixner FX (1988). Experiment Alsdan (1985), some preliminary results of height resolved measurements of trace gases, aerosol composition, cloud- and precipitation water In Unsworth MH & Fowler F (Eds.), Acid deposition at high elevation sites (pp. 375–394). Dordrecht: Springer 10.1007/978-94-009-3079-7_20

Lamb D, & Verlinde J (2011). Physics and chemistry of clouds (1st ed). New York: Cambridge University Press 10.1017/CB09780511976377

Lammel G (1995). Particulate and fog-water and cloud-water bromide in polluted air. Atmospheric Environment, 29(22), 3257–3262. 10.1016/1352-2310(95)00250-3

Lammel G, & Metzig G (1998). On the occurrence of nitrite in urban fogwater. Chemosphere, 37(8), 1603–1614. 10.1016/S0045-6535(98)00151-9

Leaitch WR, Strapp JW, Wiebe HA, & Isaac GA (1983). Measurements of scavenging and transformation of aerosol inside cumulus In Pruppacher HR, Semonin RG, & Slinn WG (Eds.), Precipitation scavenging, dry deposition, and resuspension (Vol. 1,pp. 53–66). New York: Elsevier.

Leaitch WR, Isaac GA, Strapp JW, Banic CM, & Wiebe HA (1992).The relationship between cloud droplet number concentrations and anthropogenic pollution: Observations and climatic implications. Journal of Geophysical Research, 97(D2), 2463–2474. 10.1029/91JD02739

Li T, Wang Y, Zhou J, Wang T, Ding AJ, Nie W, et al. (2017). Evolution of trace elements in the planetary boundary layer in southern China: Effects of dust storms and aerosol-cloud interactions. Journal of Geophysical Research: Atmospheres, 122, 3492–3506. 10.1002/2016JD025541

Liu XH, Wai KM, Wang Y, Zhou J, Li PH, Guo J, et al. (2012). Evaluation of trace elements contamination in cloud/fog water at an elevated mountain site in Northern China. Chemosphere, 88(5), 531–541. 10.1016/j.chemosphere.2012.02.015 [PubMed: 22503636]

Liu X, Easter RC, Ghan SJ, Zaveri R, Rasch P, Shi X, et al. (2012). Toward a minimal representation of aerosols in climate models: Description and evaluation in the Community Atmosphere Model CAM5. Geoscientific Model Development, 5(3), 709–739. 10.5194/gmd-5-709-2012

Malcolm EG, Keeler GJ, Lawson ST, & Sherbatskoy TD (2003). Mercury and trace elements in cloud water and precipitation collected on Mt. Mansfield, Vermont. Journal of Environmental Monitoring, 5(4), 584–590. 10.1039/b210124f [PubMed: 12948232]

Marinoni A, Laj P, Sellegri K, & Mailhot G (2004). Cloud chemistry at the Puy de Dome: Variability and relationships with environmental factors. Atmospheric Chemistry and Physics, 4(3), 715–728. 10.5194/acp-4-715-2004

Martens CS, Wesolowski JJ, Harriss RC, & Kaifer R (1973). Chlorine loss from Puerto-Rican and San-Francisco-Bay Area marine aerosols. Journal of Geophysical Research, 78(36), 8778–8792. 10.1029/JC078i036p08778

Maudlin LC, Wang Z, Jonsson HH, & Sorooshian A (2015). Impact of wildfires on size-resolved aerosol composition at a coastal California site. Atmospheric Environment, 119, 59–68. 10.1016/j.atmosenv.2015.08.039

Munger JW, Collett J, Daube B, & Hoffmann MR (1989a). Chemical-composition of coastal stratus clouds—Dependence on droplet size and distance from the coast. Atmospheric Environment, 23(10), 2305–2320. 10.1016/0004-6981(89)90192-3

Munger JW, Collett J, Daube BC, & Hoffmann MR (1989b). Carboxylic acids and carbonyl compounds in southern California clouds and fogs. Tellus B, 413(3), 230–242. 10.1111/j.1600-0889.1989.tb00303.x

Neale RB, Chen C-C, Gettelman A, Lauritzen PH, Park S, Williamson DL, et al. (2012), Description of the NCAR Community Atmosphere Model (CAM 5.0), NCAR Tech. Note NCAR-TN-486+STR.

Neu JL, & Prather MJ (2012). Toward a more physical representation of precipitation scavenging in global chemistry models: Cloud overlap and ice physics and their impact on tropospheric ozone. Atmospheric Chemistry and Physics, 12(7), 3289–3310. 10.5194/acp-12-3289-2012

Plessow K, Acker K, Heinrichs H, & Möller D (2001). Time study of trace elements and major ions during two cloud events at the Mt. Brocken. Atmospheric Environment, 35(2), 367–378. 10.1016/S1352-2310(00)00134-5

Polkowska Z, Blas M, Lech D, & Namiesnik J (2014). Study of cloud water samples collected over northern Poland. Journal of Environmental Quality, 43(1), 328–337. 10.2134/jeq2013.05.0172 [PubMed: 25602567]

Prabhakar G, Ervens B, Wang Z, Maudlin LC, Coggon MM, Jonsson HH, et al. (2014). Sources of nitrate in stratocumulus cloud water: Airborne measurements during the2011 E-PEACE and 2013 NiCE studies. Atmospheric Environment, 97,166–173. 10.1016/j.atmosenv.2014.08.019

Pratt KA, Fiddler MN, Shepson PB, Carlton AG, & Surratt JD (2013). Organosulfates in cloud water above the Ozarks' isoprene source region. Atmospheric Environment, 77, 231–238. https://doi.org/10.10167j.atmosenv.2013.05.011

Pruppacher HR, & Klett JD (1997). Microphysics of clouds and precipitation (2nd ed). Dordrecht, Netherlands: Kluwer Academic.

Rao X, & Collett JL (1998). The drop size-dependence of iron and manganese concentrations in clouds and fogs: Implications for sulfate production. Journal of Atmospheric Chemistry, 30(2), 273–289. 10.1023/A:1006044614291

Rehfeld S, & Heimann M (1995). Three dimensional atmospheric transport simulation of the radioactive tracers ^{210}Pb, ^{7}Be, ^{10}Be, and ^{90}Sr. Journal of Geophysical Research, 100(D12), 26,141–26,161. 10.1029/95JD01003

Russell LM, Pandis SN, & Seinfeld JH (1994). Aerosol production and growth in the marine boundary layer. Journal of Geophysical Research, 99(D10), 20,989–21,003. 10.1029/94JD01932

Russell LM, Sorooshian A, Seinfeld JH, Albrecht BA, Nenes A, Ahlm L, et al. (2013). Eastern Pacific emitted aerosol cloud experiment. Bulletin of the American Meteorological Society, 94(5), 709–729. 10.1175/Bams-D-12-00015.1

Sakashita T, Nakamura Y, & Doi M (2002). Test of wet scavenging parameterization schemes by simulation of monthly depositions of Be-7 using normally available data on environmental monitoring and local meteorology. Journal of Nuclear Science and Technology, 39(2), 180–186. 10.3327/Jnst.39.180

Schlosser JS, Braun RA, Bradley T, Dadashazar H, MacDonald AB, Aldhaif AA, et al. (2017). Analysis of aerosol composition data for western United States wildfires between 2005 and 2015: Dust emissions, chloride depletion, and most enhanced aerosol constituents. Journal of Geophysical Research: Atmospheres, 122, 8951–8966. 10.1002/2017JD026547 [PubMed: 28955601]

Schwartz SE (1986). Mass-transport considerations pertinent to aqueous phase reactions of gases in liquid-water clouds In Jaeschke W (Ed.), Chemistry of multiphase atmospheric systems (pp. 415–471). Berlin, Heidelberg: Springer 10.1007/978-3-642-70627-1_16

Sedlak DL, Hoigné J, David MM, Colvile RN, Seyffer E, Acker K, et al. (1997). The cloudwater chemistry of iron and copper at Great Dun Fell, UK. Atmospheric Environment, 31(16), 2515–2526. 10.1016/S1352-2310(96)00080-5

Seinfeld JH, & Pandis SN (2016). Atmospheric chemistry and physics (3rd ed). New York: Wiley-Interscience.

Sorooshian A, Lu ML, Brechtel FJ, Jonsson H, Feingold G, Flagan RC, & Seinfeld JH (2007). On the source of organic acid aerosol layers above clouds. Environmental Science & Technology, 41(13), 4647–4654. 10.1021/es0630442

Sorooshian A, Wang Z, Coggon MM, Jonsson HH, & Ervens B (2013). Observations of sharp oxalate reductions in stratocumulus clouds at variable altitudes: Organic acid and metal measurements during the 2011 E-PEACE campaign. Environmental Science & Technology, 47(14), 7747–7756. 10.1021/es4012383

Sorooshian A, Wang Z, Feingold G, & L'Ecuyer TS (2013). A satellite perspective on cloud water to rain water conversion rates and relationships with environmental conditions. Journal of Geophysical Research: Atmospheres, 118, 6643–6650. 10.1002/jgrd.50523

Sorooshian A, Crosbie E, Maudlin LC, Youn JS, Wang Z, Shingler T, et al. (2015). Surface and airborne measurements of organosulfur and methanesulfonate over the western United States and coastal areas. Journal of Geophysical Research: Atmospheres, 120, 8535–8548. 10.1002/2015JD023822 [PubMed: 26413434]

Sorooshian A, MacDonald AB, Dadashazar H, Bates KH, Coggon MM, Craven JS, et al. (2017). A multi-year data set on aerosol-cloud-precipitation-meteorology interactions for marine stratocumulus clouds. Figshare 10.6084/m9.figshare.5099983

Stavrakou T, Müller JF, Peeters J, Razavi A, Clarisse L, Clerbaux C, et al. (2012). Satellite evidence for a large source of formic acid from boreal and tropical forests. Nature Geoscience, 5(1), 26–30. 10.1038/NGEO1354

Stephens GL, & Haynes JM (2007). Near global observations of the warm rain coalescence process. Geophysical Research Letters, 34, L20805. 10.1029/2007GL030259

Straub DJ, Lee T, & Collett JL (2007). Chemical composition of marine stratocumulus clouds over the eastern Pacific Ocean. Journal of Geophysical Research, 112, D04307 10.1029/2006JD007439

Sun M, Wang Y, Wang T, Fan S, Wang W, Li P, et al. (2010). Cloud and the corresponding precipitation chemistry in south China: Water-soluble components and pollution transport. Journal of Geophysical Research, 115, D22303. 10.1029/2010JD014315

Sun L, Wang Y, Yue T, Yang X, Xue L, & Wang W (2015). Evaluation of the behavior of clouds in a region of severe acid rain pollution in southern China: Species, complexes, and variations. Environmental Science and Pollution Research, 22(18), 14,280–14,290. 10.1007/s11356-015-4674-5

Talbot RW, Mosher BW, Heikes BG, Jacob DJ, Munger JW, Daube BC, et al. (1995). Carboxylic-acids in the rural continental atmosphere over the eastern United-States during the Shenandoah Cloud and Photochemistry Experiment. Journal of Geophysical Research, 100(D5), 9335–9343. 10.1029/95JD00507

van Pinxteren D, Fomba KW, Mertes S, Müller K, Spindler G, Schneider J, et al. (2016). Cloud water composition during HCCT-2010: Scavenging efficiencies, solute concentrations, and droplet size dependence of inorganic ions and dissolved organic carbon. Atmospheric Chemistry and Physics, 16(5), 3185–3205. 10.5194/acp-16-3185-2016

Wang HL, & Feingold G (2009). Modeling mesoscale cellular structures and drizzle in marine stratocumulus. Part I: Impact of drizzle on the formation and evolution of open cells. Journal of the Atmospheric Sciences, 66(11), 3237–3256. 10.1175/2009JAS3022.1

Wang H, Easter RC, Rasch PJ, Wang M, Liu X, Ghan SJ, et al. (2013). Sensitivity of remote aerosol distributions to representation of cloud-aerosol interactions in a global climate model. Geoscientific Model Development, 6(3), 765–782. 10.5194/gmd-6-765-2013

Wang Z, Sorooshian A, Prabhakar G, Coggon MM, & Jonsson HH (2014). Impact of emissions from shipping, land, and the ocean on stratocumulus cloud water elemental composition during the 2011 E-PEACE field campaign. Atmospheric Environment, 89, 570–580. 10.1016/j.atmosenv.2014.01.020

Wang Z, Mora Ramirez M, Dadashazar H, MacDonald AB, Crosbie E, Bates KH, et al. (2016). Contrasting cloud composition between coupled and decoupled marine boundary layer clouds. Journal of Geophysical Research: Atmospheres, 121,11,679–11,691. 10.1002/2016JD025695

Watanabe K, Ishizaka Y, & Takenaka C (2001). Chemical characteristics of cloud water over the Japan Sea and the Northwestern Pacific Ocean near the central part of Japan: Airborne measurements. Atmospheric Environment, 35(4), 645–655. 10.1016/S1352-2310(00)00358-

Weathers KC, Likens GE, Bormann FH, Bicknell SH, Bormann BT, Daube BC, et al. (1988). Cloudwater chemistry from 10 sites in North-America. Environmental Science & Technology, 22(9), 1018–1026. 10.1021/es00174a004

Wieprecht W, Acker K, Mertes S, Collett J, Jaeschke W, Bruggemann E, et al. (2005). Cloud physics and cloud water sampler comparison during FEBUKO. Atmospheric Environment, 39(23–24), 4267–4277. https://doi.org/10.1016Zj.atmosenv.2005.02.012

Wilkinson J, Reynolds B, Neal C, Hill S, Neal M, & Harrow M (1997). Major, minor and trace element composition of cloudwater and rainwater at Plynlimon. Hydrology and Earth System Sciences, 7(3), 557–569. 10.5194/hess-1-557-1997

Wonaschütz A, Coggon M, Sorooshian A, Modini R, Frossard AA, Ahlm L, et al. (2013). Hygroscopic properties of smoke-generated organic aerosol particles emitted in the marine atmosphere. Atmospheric Chemistry and Physics, 73(19), 9819–9835. 10.5194/acp-13-9819-2013

Wood R (2005). Drizzle in stratiform boundary layer clouds. Part 1: Vertical and horizontal structure. Journal of the Atmospheric Sciences, 62(9), 3011–3033. 10.1175/Jas3529.1

Wood R (2006). Rate of loss of cloud droplets by coalescence in warm clouds. Journal of Geophysical Research, 7 7 7, D21205. 10.1029/2006JD007553

Wood R (2012). Stratocumulus clouds. Monthly Weather Review, 740(8), 2373–2423. 10.1175/MWR-D-11-00121.1

Youn JS, Crosbie E, Maudlin LC, Wang Z, & Sorooshian A (2015). Dimethylamine as a major alkyl amine species in particles and cloud water: Observations in semi-arid and coastal regions. Atmospheric Environment, 722,250–258. 10.1016/j.atmosenv.2015.09.061

Key Points:

- Three characteristic in-cloud vertical concentration profiles are identified: those that peak at the base, middle, and top of cloud
- Nonreactive surface-derived species present the in-cloud vertical concentration profiles that are most influenced by rainout
- Rainout loss frequency is greatest at cloud base for moderate-drizzling thick clouds, and at cloud top for light-drizzling thin clouds

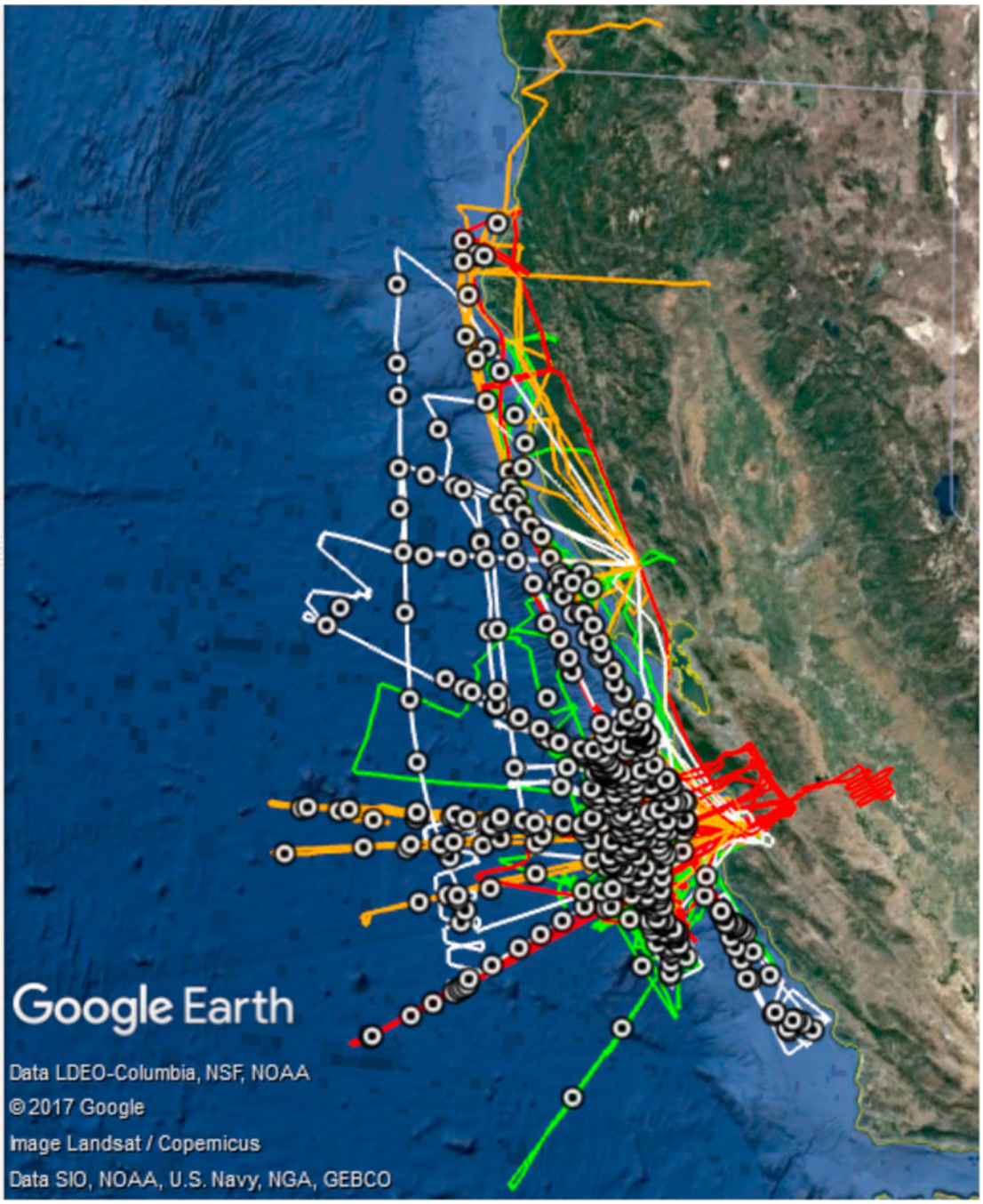

Figure 1.
Flight tracks of the four missions from which data are analyzed (green = E-PEACE 2011, orange = NiCE 2013, red = BOAS 2015, white = FASE 2016), and sample-averaged locations denoting where each cloud water sample was collected (circular markers). Only research flights that were over the ocean at any point in that flight are shown.

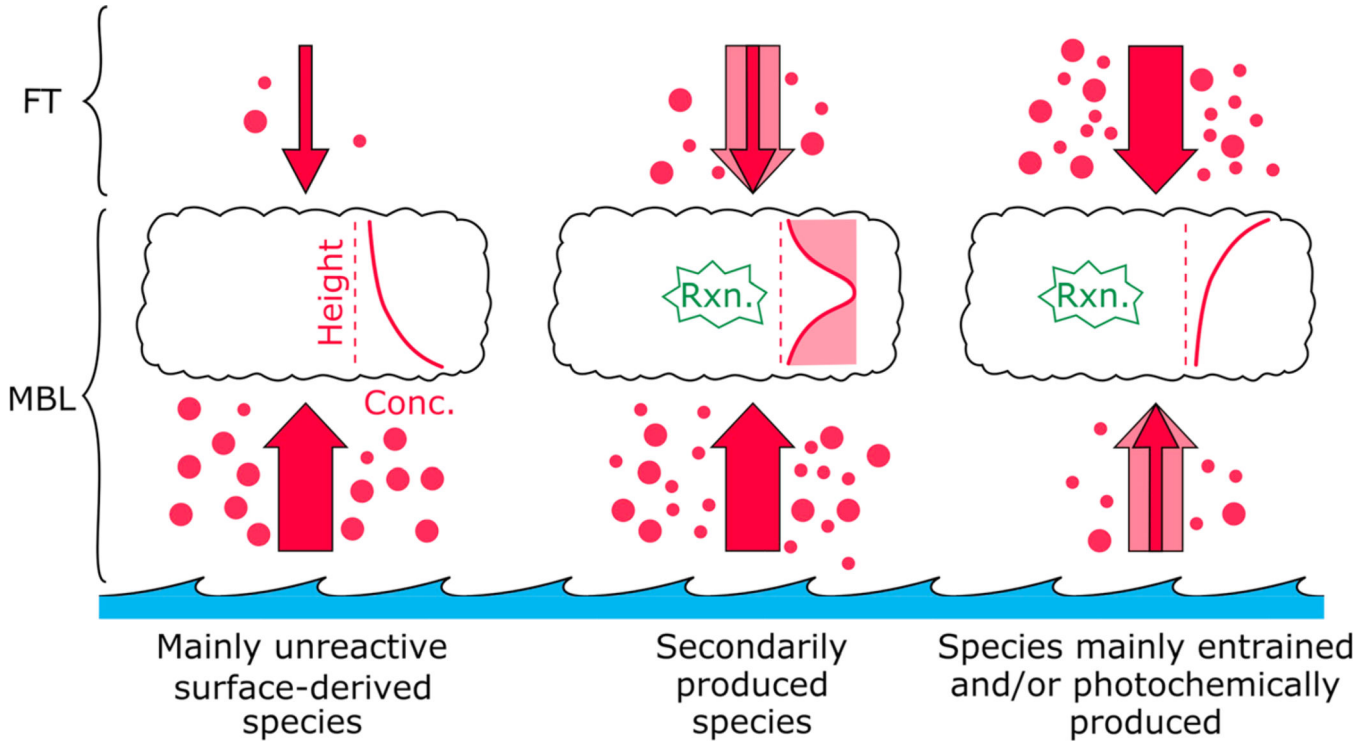

Figure 2.

Characteristics governing the three idealized in-cloud air-equivalent concentration vertical profiles. FT = free troposphere, MBL = marine boundary layer, Rxn. = secondary chemical production mechanism in droplets. The thickness of the arrow represents the magnitude of influence from surface or free tropospheric sources. The small circles represent gases; the large circles represent aerosols. The shaded arrow thicknesses and concentration profiles illustrate variability in relative source strengths and concentration profiles.

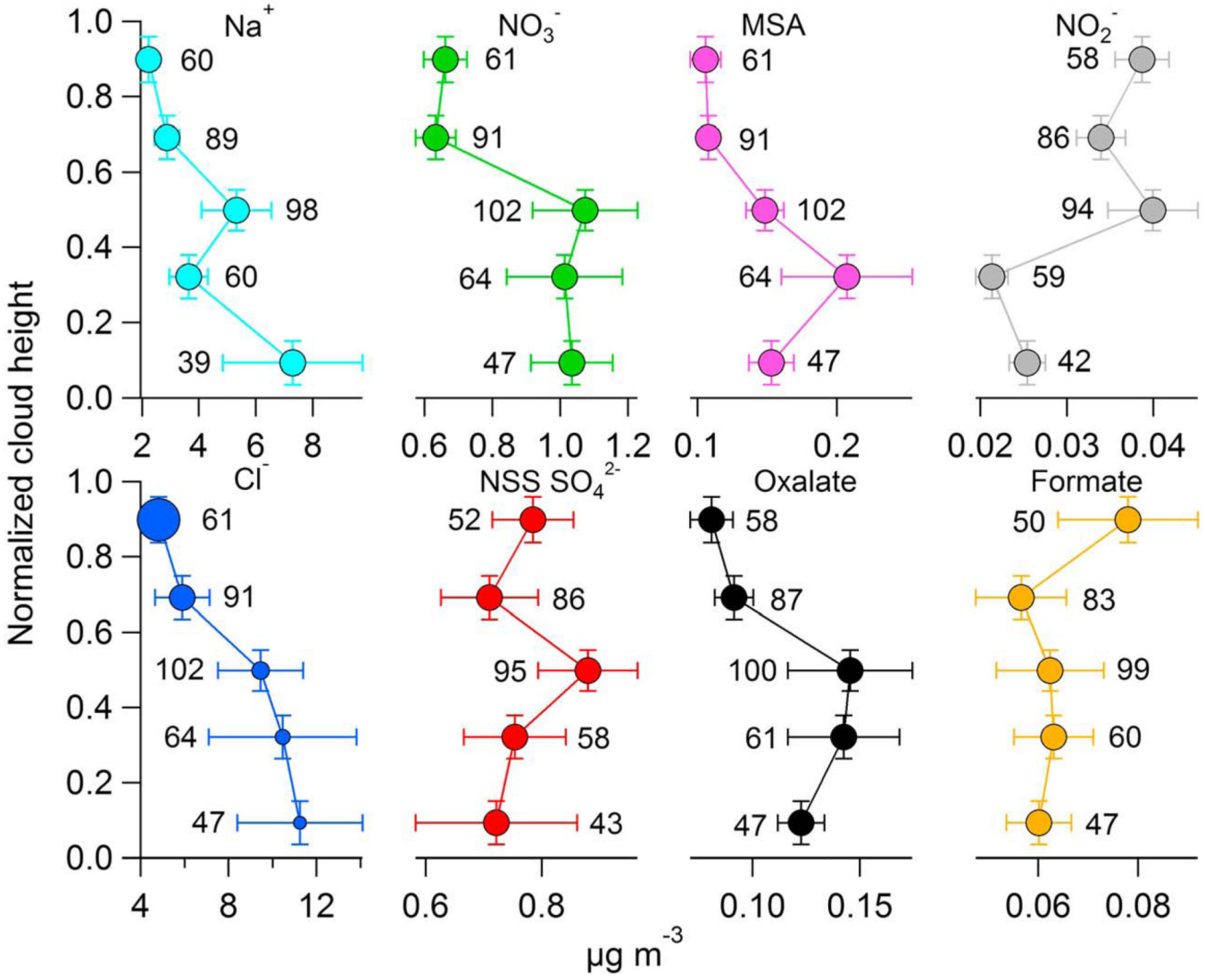

Figure 3.

In-cloud vertical concentration profiles of selected species using the cumulative approach, that is, vertically averaged means of air-equivalent mass concentrations from all samples collected during the four field campaigns. Marker sizes for the Cl^- profile are proportional to the Cl^-:Na^+ mass concentration ratio, ranging from 1.72 in the bottom fifth to 1.86 in the top fifth of clouds. The vertical error bars represent the standard deviation of normalized cloud height. The horizontal error bars represent one tenth of the standard deviation of air-equivalent concentration. The numbers next to the horizontal error bars are the number of data points used for calculations of that vertical bin.

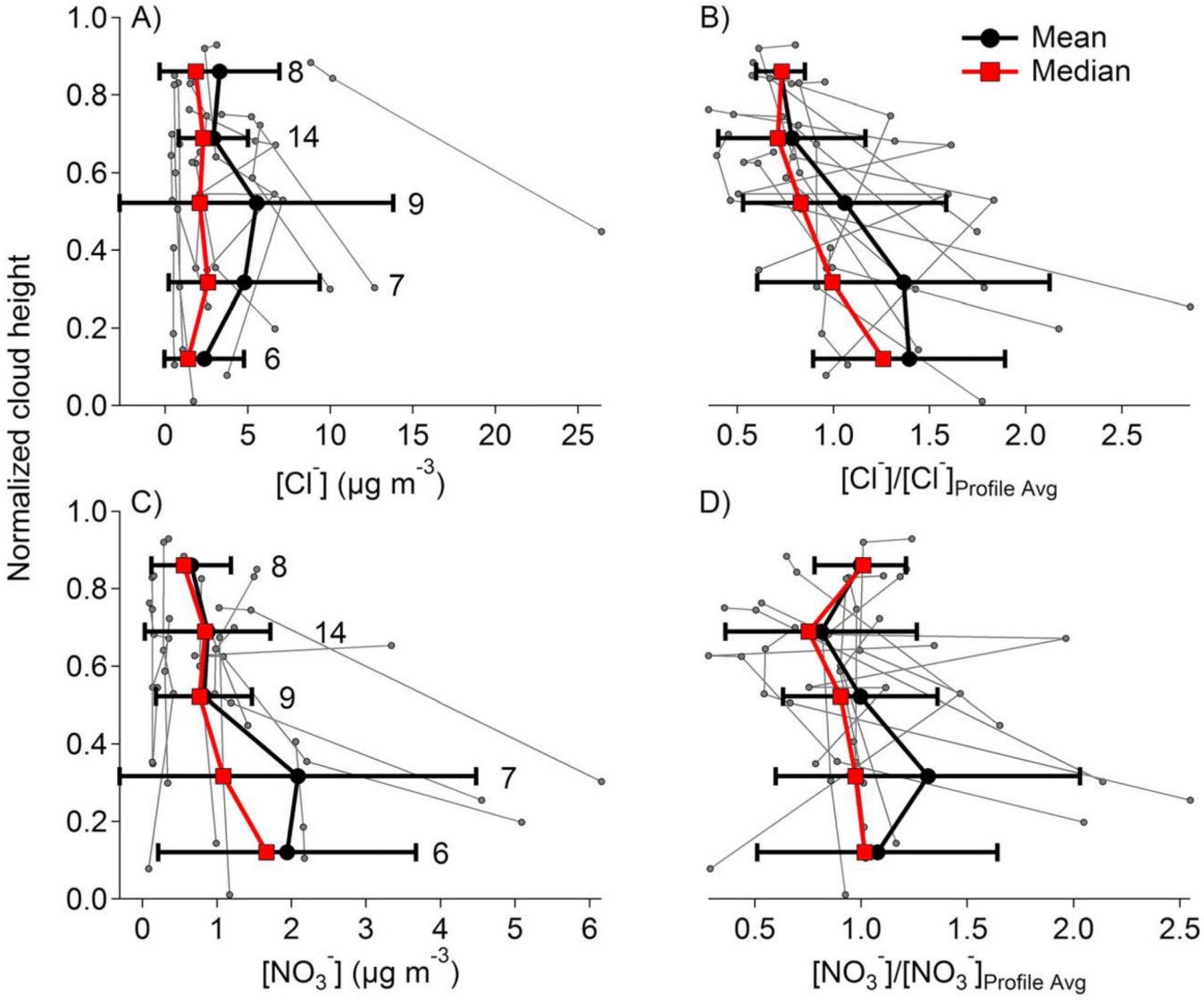

Figure 4.

Comparison of different characteristic profiles obtained using the case study approach. The thick black lines represent means with error bars showing standard deviation. The thick red lines represent medians. The thin gray lines represent the 11 individual profiles. (a and c) Vertical air-equivalent mass concentration profiles of Cl^- and NO_3^-, respectively. (band d) Vertical profiles of normalized concentration of Cl^- and NO_3^-, respectively. Normalization of a given profile is calculated with respect to the average columnar concentration of an entire profile. The number of data points used for each bin is shown next to the error bars.

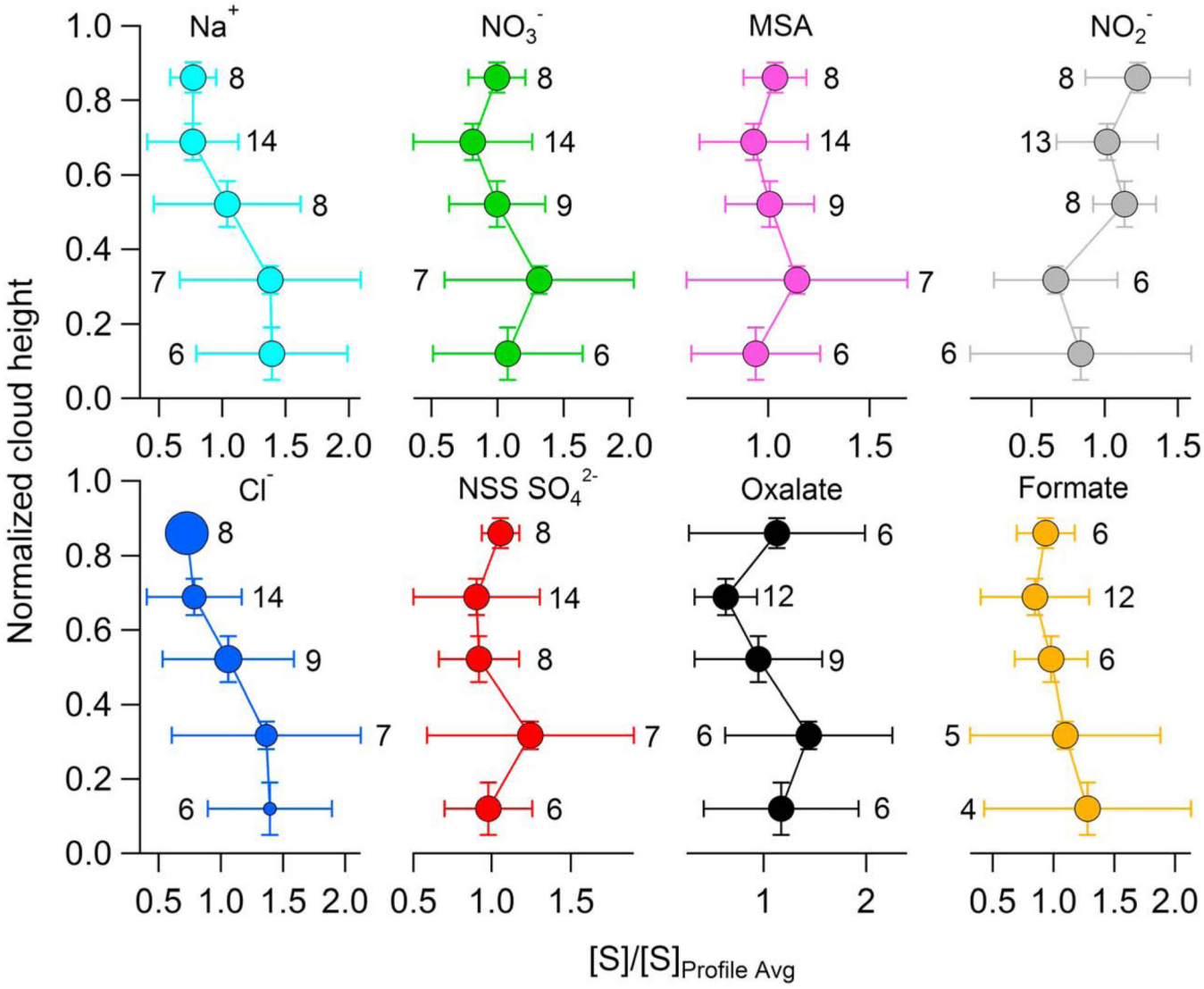

Figure 5.

In-cloud vertical profiles of selected species using the case study approach. The profiles represent the mean of the 11 case study air-equivalent concentration profiles after each profile was normalized by the average columnar air-equivalent concentration of that profile. The horizontal and vertical error bars represent standard deviations of the normalized cloud height and normalized air-equivalent concentration, respectively. The numbers next to the horizontal error bars represent the number of data points used for calculations for a particular vertical bin. Marker sizes for the Cl^- profile are proportional to the Cl^-:Na^+ mass concentration ratio, ranging from 1.66 in the bottom fifth to 2.17 in the top fifth of clouds.

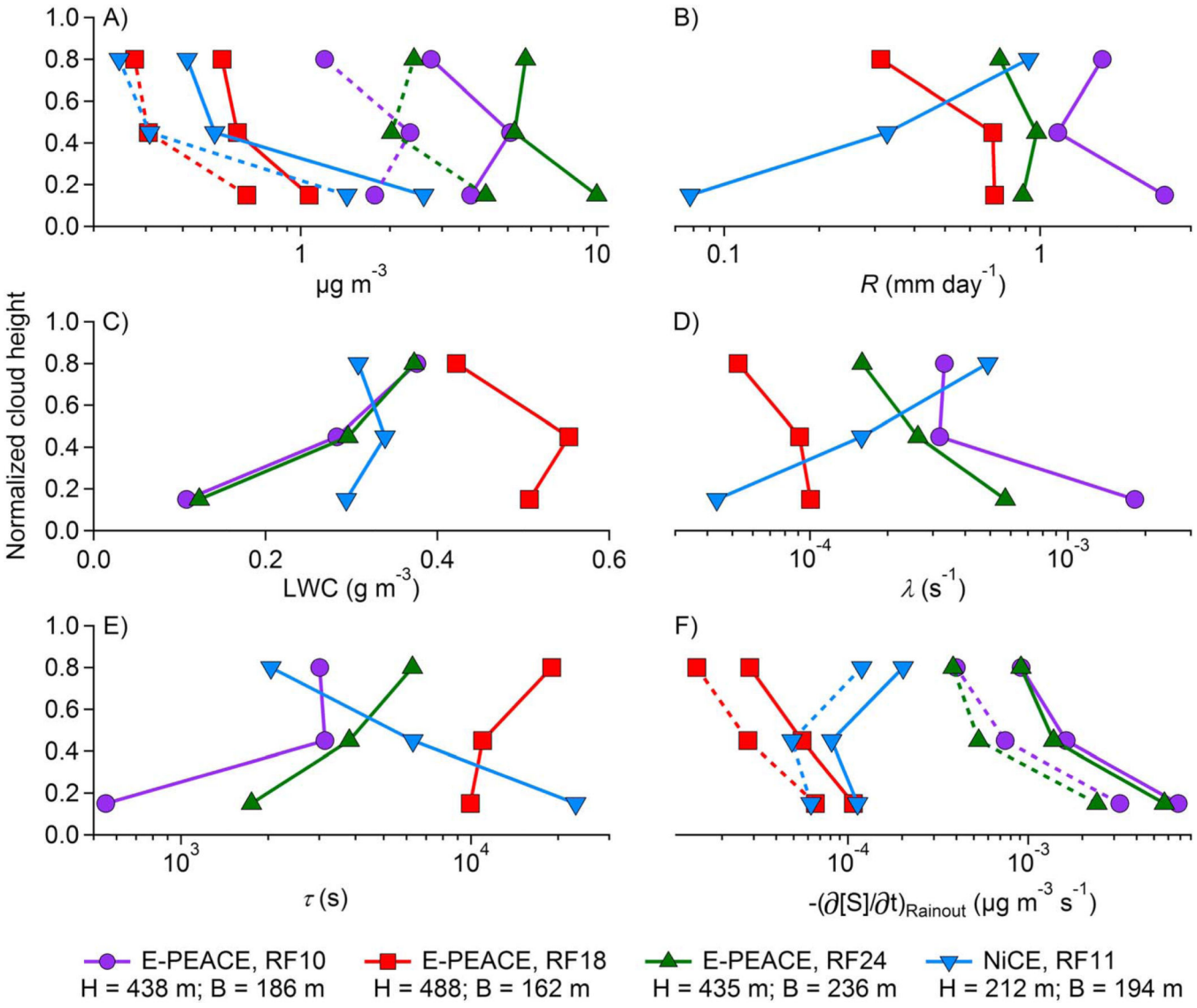

Figure 6.

Vertical profiles of (a) Cl^- and Na^+ air-equivalent mass concentrations, (b) rain rate (R), (c) LWC, (d) rainout loss frequency (λ), (e) rainout lifetime (τ), and (f) loss rate of Cl^- and Na^+ concentration due to rainout. In panels a and f, the solid and dashed lines represent Cl^- and Na^+, respectively. H = cloud depth; B = cloud base.

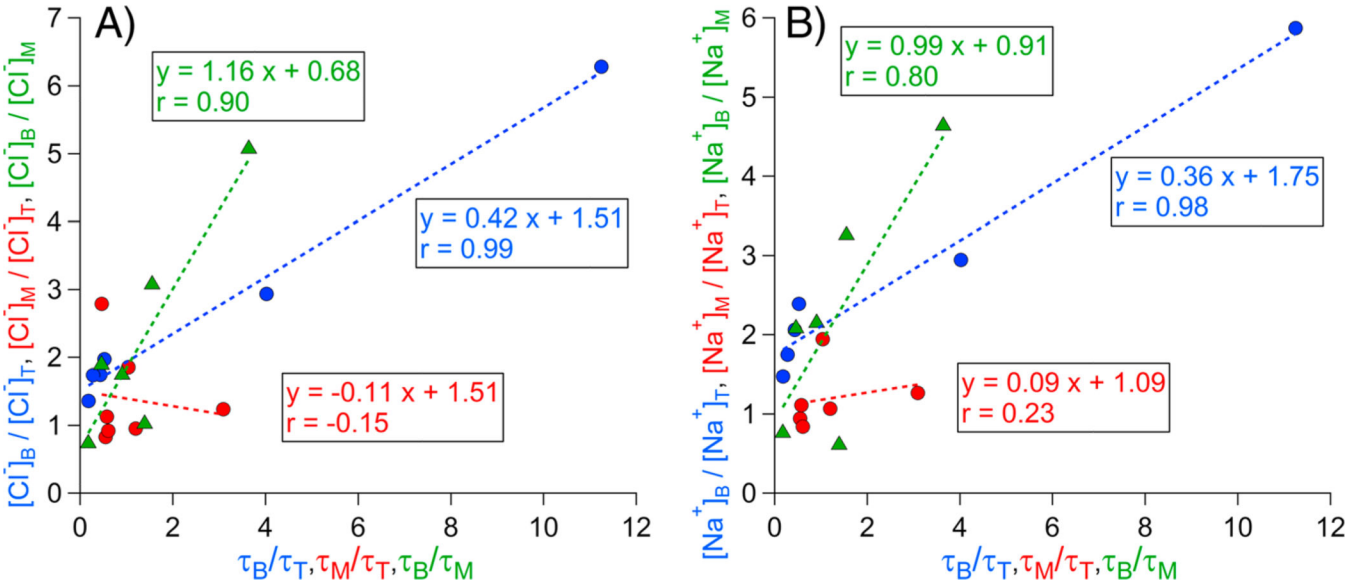

Figure 7.

(a and b) Relationship between the species air-equivalent concentration ratio (Cl^- and Na^+, respectively) and rainout lifetime (τ) ratio between two different thirds of clouds. Markers are shown separately for comparisons between the bottom and top third (B/T, blue), middle and top third (M/T, red), and bottom and middle third (B/M, green).

Table 1

Details of the Four Field Campaigns Addressed

Field campaign	Dates (d/m/y)	No. of flights	No. of samples	Sample altitude range (m)
Eastern Pacific Emitted Aerosol Cloud Experiment (E-PEACE)	8/7/2011–18/8/2011	30	82	124–805
Nucleation in California Experiment (NiCE)	8/7/2013–7/8/2013	23	119	119–998
Biological and Oceanic Atmospheric Study (BOAS)	2/7/2015–24/7/2015	15	29	131–941
Fog and Stratocumulus Evolution Experiment (FASE)	18/7/2016–12/8/2016	16	155	81–728

Table 2

Summary of the Coefficients of the Linear Regression Equation

	Bottom/Top					Middle/Top					Bottom/Middle				
Species	***m***	***b***	***r***	***n***	***p***	***m***	***b***	***r***	***n***	***p***	***m***	***b***	***r***	***n***	***p***
Na	0.36	1.74	0.98	6	< 0.01	0.09	1.09	0.23	6	0.66	0.99	0.91	0.80	6	0.06
Cl^-	0.42	1.51	0.99	6	< 0.01	−0.11	1.51	−0.15	7	0.75	1.16	0.68	0.90	6	0.01
NO_3^-	0.31	1.14	0.72	6	0.11	−0.19	1.34	−0.30	7	0.51	1.13	0.27	0.94	6	< 0.01
NSS SO_4^{2-}	0.22	1.07	0.75	6	0.09	−0.08	1.01	−0.42	6	0.41	0.99	0.21	0.97	6	< 0.01
MSA	0.21	0.79	0.85	6	0.03	−0.03	1.07	−0.08	7	0.86	0.61	0.43	0.97	6	< 0.01
Oxalate	0.21	2.42	0.38	5	0.53	−1.19	4.41	−0.32	5	0.60	0.76	1.58	0.35	5	0.56
NO_2^-	0.13	0.45	0.70	6	0.12	0.15	0.86	0.24	7	0.60	0.27	0.66	0.28	6	0.59
Formate	0.18	1.37	0.39	5	0.52	−0.14	1.22	−0.47	4	0.53	0.42	1.95	0.33	3	0.79
Fe	0.23	2.27	0.49	6	0.32	−0.25	1.70	−0.50	5	0.39	1.22	0.87	0.75	6	0.09

Note. The table is an extension of Figure 7, showing the coefficients of the linear regression equation of the form $y = mx + b$, where x is the ratio of lower-to-higher altitude values of τ and y is the ratio of lower-to-higher altitude values for species air-equivalent concentrations. The number of data points is denoted as n. Correlation coefficients (r) and p values are also reported.